# Evaporator and type I cooling tubes and their connections for the ATLAS phase II barrel strip tracker

## Part I: Requirements and Specifications

Richard Bates, Richard French, Robert Gabrielczyk, Martin Gibson, Tim Jones, John Noviss, Hector Marin-Reyes, John Mathieson, Ian Mercer, Steve Snow, Peter Sutcliffe, Georg Viehhauser, Ian Wilmut (to be completed)

Draft v2.3

Table of Contents

# 1 Introduction

This report is the first in a series summarizing our R&D on metallic cooling tubes for the barrel strip staves of the ATLAS phase II upgrade and the tracker-internal transfer pipes (type I pipes). This report lays down the requirements we have identified for these tubes and the specifications we derived from them. It will be followed by two reports outlining the R&D on bending and joining techniques [1], and our plans for implementation in the final tracker, and describing the performance verification of these designs [2].

As will be discussed throughout this document metallic tubes appear to us the most promising candidates for the evaporator and transfer pipes with high uniformity, good formability, high cross-wall heat conductivity and due to their widespread use and large range of well-established joining technologies. All these considerations motivate our choice of tube materials from this category.

This report starts with a short description of the ATLAS barrel strip project and its cooling aspects. The main part is then the discussion of requirements and specifications, which is complemented by an extensive set of appendices detailing the arguments in this report.

# 2 Cooling for the ATLAS barrel strip upgrade

The mechanical design of the ATLAS upgrade staves is described in ref. [3]. As discussed in Appendix A we expect the maximum total heat to be removed from a stave (short-strip), including safety factors, to be 140 W. The maximum design evaporation temperature of the future ATLAS cooling system is -35°C, driven by the need to maintain thermal stability in the pixel system [4]. For detailed calculations on the thermal performance of the barrel strip staves see ref. [3]. According to the LOI layout [5] there will be 216 short-strip and 256 long-strip stave staves, the latter with a smaller power load (50 to 75 W), mostly due to less on-detector front-end electronics channels. However, we plan to have one common stave core design for short- and long-strip staves, and therefore the cooling tube dimensions will be determined by the high power case.

The cooling in the future ATLAS tracker will be evaporative $CO_2$ cooling following the 2-Phase Accumulator-Controlled Loop (2PACL) principle pioneered by the AMS and LHCb VELO experiments [6]. The latent heat of $CO_2$ at -35°C is 313 kJ/kg. Assuming boiling between an initial vapour quality $x = 0$ and a final vapour quality $x = 0.5$, the required mass flow per stave is 0.9 g/s. In the ATLAS tracker the evaporators are part of manifolds with no active flow control. Therefore the actual nominal mass flow through each evaporator needs to be bigger than this to ensure that the required flow is supplied even when the impedance in parallel evaporators drops because of a different load condition. This flow overhead can be reduced by capillaries in series before the evaporators. Without detailed calculations we set the pressure drop ratio between the capillaries and the evaporators under nominal load condition (140 W) to 10:1. In this case, if we assume the entire pressure drop to be momentum pressure drop due to evaporation caused by the heat load (no frictional pressure drop) the required overhead flow rate for infinitely large manifolds would be 10%, with smaller overheads required for smaller manifolds. Without detailed calculations or measurements we therefore assume a nominal mass flow in each evaporator of 1 g/s as a safe choice.

Figure 1 shows an overview of the cooling pipework. From the cooling plants in USA15 the coolant is transferred in concentric feed and return lines to Patch Panel 2 (PP2), which is located at the end of the ATLAS barrel, just outside of the inner muon station. In this location a first level of manifolding will take place. From PP2 lines will penetrate the inner muon layer and run radially inwards on the calorimeter endplate to the chamfer region and the start of the bore for the inner tracker. These lines are referred to as type II pipes and have not been designed, but it is likely that they will be individual lines with a common set of insulation (active or passive). At the cryostat chamfer the type II pipes will connect to Patch Panel 1 (PP1), which is the connector field at the end of the tracker. Immediately behind PP1 the cooling pipes break through the tracker thermal enclosure, so that from then on pipes do not need thermal insulation. The internal pipes between PP1 and the strip tracker barrel end are referred to as type I pipes. Within their length a second level of manifolding to individual staves is required, as well as a section of small diameter capillary in the feed line, which is needed to maintain a balanced flow in the branches of the manifolds for all load conditions. The type I services run from PP1 along the outside of the endcaps to the service gap between the barrel and the endcap, where they run radially to the connection with the stave. PP1 and the type I services are part of the strip barrel service modules.

An important design parameter for the cooling system is the pressure drop in the evaporator and the return lines. This must be limited to allow for the operation of the pump with a sufficient margin to the freezing point of $CO_2$ at -56°C. Currently we allocate a pressure drop equivalent to a temperature drop of 10°C to the evaporator and all return lines up to the plant. This is divided into a 3°C temperature drop along the evaporator, a pressure drop equivalent to 3°C from the end of the stave to PP2, and another pressure drop equivalent to 3°C from PP2 to the plant. This will drive the requirements for the inner pipe diameters in the different sections.

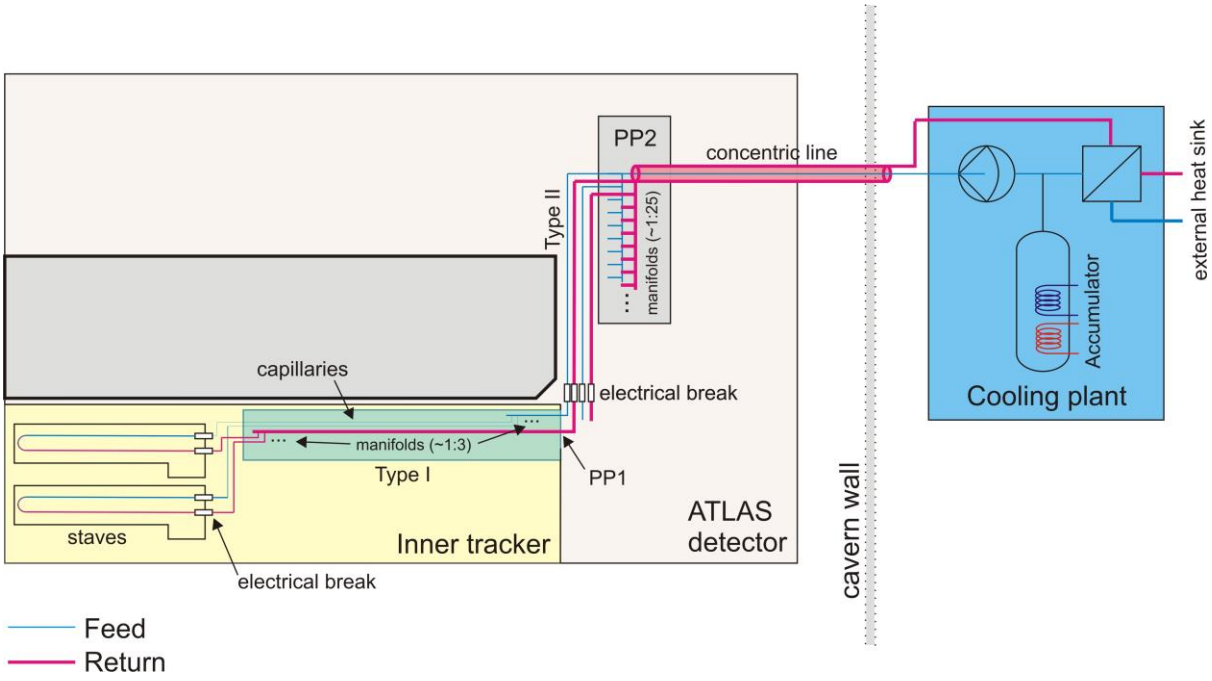


**Figure 1: Schematic overview of the cooling pipework for the barrel strip system for the ATLAS phase II upgrade. Feed lines in blue, return lines in red.**

An exploded view of the strip stave design is given in Figure 2. Within the barrel strip staves the cooling pipe is glued into blocks made of carbon foam (supplied by Allcomp 0.45 g/cm$^3$, thermal conductivity about 80 W/Km) with high thermal conductivity, which form part of the core of the carbon fibre sandwich structure in the stave. The on-detector cooling tube will be embedded into the stave core as part of the stave assembly process. In preparation for the stave assembly the tube will be bent to shape (see ref. [1]), equipped with temporary fittings used during assembly testing, and tested. Two tube geometries are currently considered, one, which has a straight 'U' shape (Figure 4), and the other, where the tube folds back to a second, short 'U', which provides dedicated cooling for the End-Of-Stave (EOS) card. It will depend on the thermal performance of the exact design of the EOS card and their components to decide whether the former tube geometry will be sufficient.

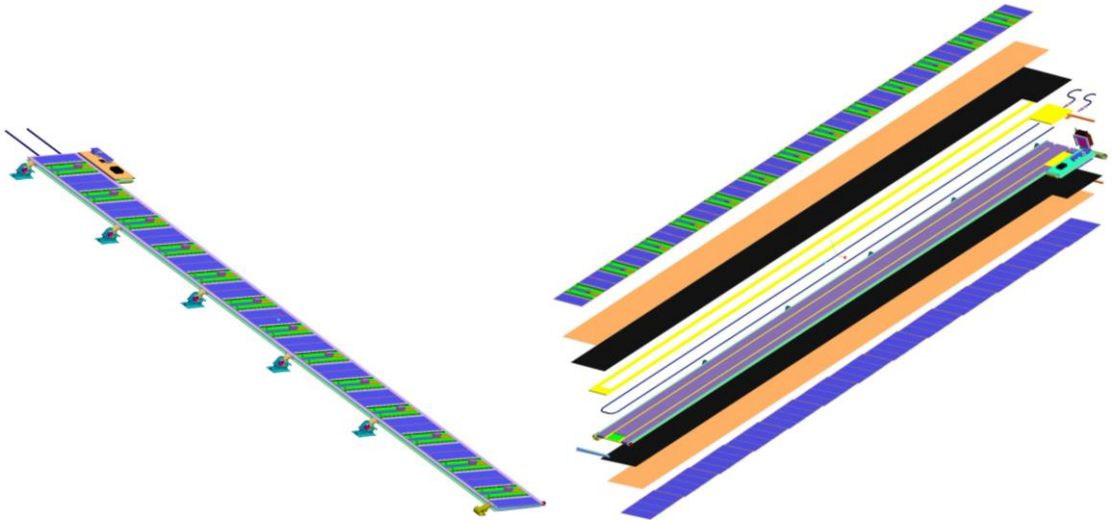

Figure 2: ATLAS upgrade strip stave design (left) and exploded view (right) with single 'U' shaped cooling tube and the electrical breaks embedded into the stave core. The left view shows straight cooling tubes out of the stave, whereas the right shows the bend outer sections for strain relief and tool access, as planned for the final design.

Figure 3: Cross-section of barrel strip stave. Cooling tube is embedded in high-conductivity carbon foam (yellow).

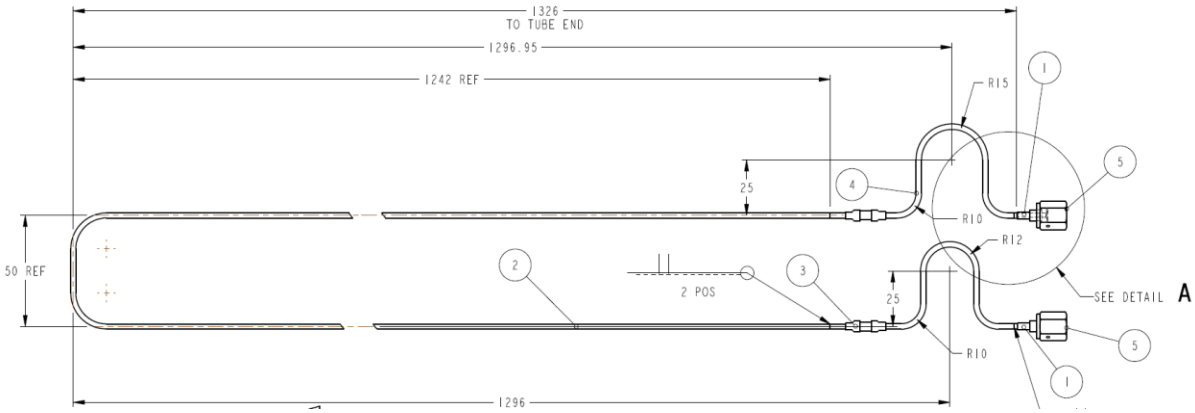


Figure 4: Stave tube assembly (dimensions in mm) for straight 'U' shape. 1-VCR gland, 2-cooling tube, 3-electrical break assembly, 4-outer tube, 5-VCR female nut.

A further design choice will be the location of the electrical break close to the end of the stave. This break is required by the electrical grounding and shielding strategy as explained in section 3.14. One solution studied for this break is to incorporate it into the stave end. If this is not possible, it will be located in the service gap, close to the end of the stave. For further discussion of the technology of the electrical break see ref. [1].

The type I services including the cooling tubes will be contained in the barrel strip type I service module (Figure 5). These services will connect to the individual staves at the stave end, from where they run radially out in the service gap between the strip barrel and in front of the strip endcaps. The

tubes will not run straight radially but feature several bends for stress relieve and tooling access. Close to the inner wall of the outer cylinder they bend around the strip end cap and run within the service module container to the end of the tracker where they terminate in the PP1 connector area. To limit the number of cooling connections at PP1 a small amount of manifolding is foreseen within the tracker (1:2 to 1:4, depending on the power on the individual staves).

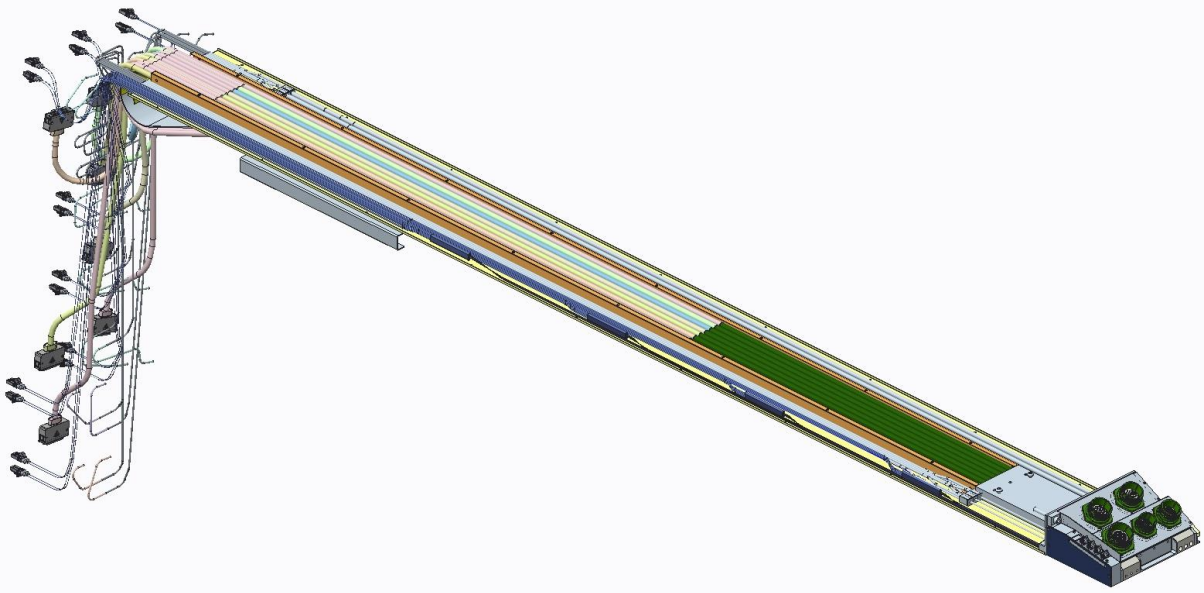

**Figure 5: Barrel strip type I service module (container lid removed).**

After the mounting of modules onto the stave core the full functionality of the stave will need to be verified at the assembly site. For the connection to the cooling system during these tests temporary fittings will be used. Completed staves will then be shipped to the integration site at CERN, where the staves will get end-inserted into the barrel strip support structure. A quick functionality check with a temporary cooling system connection might be required, before the final connection of the on-detector cooling tube to the type I services. This connection will only be broken in the rare case that a stave develops a serious fault late in the integration sequence and needs to be replaced.

# 3 Requirements

## 3.1 Standards and their application to barrel strip pipework

For the design of typical industrial pressurised gas installations there are a number of national and international codes and standards[1]. These codes summarize many years of tried and tested methods built upon a theoretical basis. These standards are guidelines for designs and methods, but, on their own, not legally binding requirements. However, in many applications it would be usual to design directly to these standards and then have the system certified to conform to them.

For the ATLAS tracker update these codes represent a robust basis from which to start the design – however, as many of our requirements and conditions are outside the scope of these standards they can't be used directly. Our system will not require certification, but will need acceptance by CERN safety, and it is likely that this will require that we have designed and built the cooling system in accordance with international standards.

In addition to standards on pressure handling extensive standards exist describing a range of topics which are relevant for this document such as weld defects, weld QA, and material properties. Again, in many cases our application is not directly covered by the scope of these standards. Nevertheless, much of the material is relevant and we have used the standards heavily in defining the project processes. Exactly how the standards have been used is explained in each section, giving references to the appropriate standards and the reasons for the inclusion or exclusion should we fall outside the standard's scope.

## 3.2 Design pressure

The present guidance for designing pressure vessels in Europe can be found in the Pressure Equipment Directive 97/23/EC (PED), and the normative European standard (EN 13445). Two other interesting guides are the now obsolete British standard PD5500 and the ASME Boiler and Pressure Vessel (BPV) code.

All of these standards focus on the design of pressure vessels and start with a definition of a pressure vessel. The numerical definitions vary somewhat, but all are based around a pressure-volume factor (15 PSIg in ASME, 0.5 barl in the PED). All codes also make a distinction between the piping that serves a vessel and the vessel itself. We understand the cooling tubes (evaporators and type I tubes) within the ATLAS tracker to be categorised as piping rather than a pressure vessel. Because of this the relevant standard is EN13445 which describes the design of pressure handling pipework. Again the ASME BPV code is still the equivalent US document.

EN13445 assumes that the pipe is retained along its length with pipe clips at intervals. This is not the case for the cooling tube in a barrel strip stave. This tube is glued into a cooling channel made of carbon foam. The calculations in EN13445 are therefore not directly applicable, but Annex B discusses calculation by analysis, which is. We calculated the wall thickness for our cooling tubes based on these standards but backed up the results of these calculations with FEA studies of the constrained tube (section 4.6).

[1] For a listing of standards see Appendix D.

For our definitions of the pressure requirements we follow the definitions in the PED and EN 13445. The definitions are consistent with the approach used in the design and manufacture of the ATLAS IBL $CO_2$ cooling system [7].

In the PED the defining pressure is the *maximum allowable pressure* $P_s$, which is defined as "Maximum allowable pressure means the maximum pressure for which the equipment is designed, as specified by the manufacturer." We use this pressure to calculate the wall thickness of tubes in the system using the subsequent standard EN 13480 (see section 4.6.1). The ASME BPV code defines the *maximum allowable working pressure (MAWP)*, which is equivalent to the *maximum allowable pressure* in the EN. It further defines the *maximum operating pressure (MOP)*, which should be less or equal to the MAWP, but it does not prescribe their ratio. EN 13445 also specifies the test pressure to which all components of a pressure system need to be tested hydraulically to be $1.43 \times P_s$ (ASME BPV prescribes hydraulic test to 1.5×MAWP). As will be discussed in Appendix E and F the safety factors required by these standards for the wall thickness dimensioning put this test pressure well within the pressure containment capabilities of the system.

In each closed volume the pressure of a fluid increases as a function of the temperature if heated actively or by the environment. The accumulator in a 2PACL system is designed to contain all liquid in the system, as well as allowing control of the temperature up to 35°C. For an appropriately dimensioned accumulator volume this would result in an operating pressure of 110 $bar_a$. Any higher pressures will be limited by pressure safety valves. Within the rest of the system the operating pressure will be given by the maximum discharge pressure of the pumps, which is defined by the maximum saturation pressure of the $CO_2$ fluid, which is 65 $bar_a$ (during start-up the system is flooded with warm liquid at up to 25°C), plus the pump head required to drive the fluid through the system (which is expected to be in the order of 25 $bar_a$). Pump discharge pressure will be limited to similar values as the pressure limit for the accumulator. The pressure in each section which can be closed off needs to be limited by a burst disc. The burst limit for these discs should be higher than the regular operating pressures and a convenient pressure limit is 130 $bar_g$, for which commercial standard burst discs do exist []. Although we do not plan that this limit will be reached during operation we do allow for such a condition and this defines therefore the maximum allowable pressure $P_s$ to be 130 $bar_a$. This means that all components need to be tested hydraulically to 186 $bar_a$.

## 3.3 Leak rate

While design pressure requirements for pressurized systems are strongly regulated there exist no standardized regulations prescribing the leak rates throughout the system. There are also no other strong requirements on the leak rate of the future ATLAS $CO_2$ cooling system, like cost or environmental concerns or a concern of contamination of the tracker volume, other than that a low leak rate reflects diligent engineering of the pipework and connections as required for a system at considerable pressure. We therefore derive a leak rate limit for the components in the future cooling system from a target overall allowable leak rate of the future cooling system, which we set to 5% of the total coolant in the system per year. Assuming that the total amount of coolant in the tracker is 1000 kg, the total leak rate of the system would be 0.5 mbarl/s for a leak at regular operation (-35°C, 12 $bar_a$). Assuming $10^3$ internal circuits this translates into a leak rate of $5 \times 10^{-4}$ mbarl/s per circuit, and, assuming $10^4$ joints, a leak rate of $5 \times 10^{-5}$ mbarl/s per joint. As the leak rate is defined from an

integrated leak rate target, the component leak rate has to be achieved under standard operating conditions (-35°C and 12 $bar_a$).

## 3.4 Failure rate

Due to the complex nature of the tracker internal cooling circuits (manifolds, capillaries, reduction of diameters in critical areas while maintaining maximum design pressure drops, electrical breaks) there is a large number of joints within the tracker (on average about 20 per circuit, of the order of $10^4$ for the whole tracker). As these joints will be inaccessible with any reasonable effort, they have to have excellent reliability (failure rate of 1 in $10^5$ for a 10% probability of a failure somewhere in the system[2]).

Failure here is defined as the development of a leak rate which would require disconnection of the circuit and its associated manifolds. We define this leak rate to be above 100 kg/y or 1 mbarl/s at the regular operating point, which is significantly above the leak rate specification per joint as outlined in the previous section. This failure rate needs to be achieved over the full lifetime of the phase II upgrade, including handling during assembly and integration, and all thermal cycling.

If one restricts the analysis to the final connection of staves to the type I services (order of $10^3$ connections) the failure rate needs to be 1 in $10^4$ for a 10% probability of a failure in the system. To demonstrate such a failure rate with 90% confidence $2.3\times10^4$ joints without failure would need to be demonstrated.

## 3.5 Certification

Pressure vessels such as gas canisters need to be certified by an appropriate body for their safety. Piping systems such as those within the tracker volume do not require certification as they are classified as piping. Apart from the probably increased administrative overhead in case of certification by another body the only significant difference is who has the responsibility for the safety of the system. Having a non-certified system means that solely the engineers designing the system are responsible for its performance and safety.

## 3.6 Environment

### 3.6.1 Temperature

The materials of the components of the cooling circuit must not be affected by the low temperatures of the cooling system. The target maximum evaporation temperature for the future cooling system on the detector will be -35°C. Due to the pressure drops in the on-detector evaporator and the return line pipe work the temperature of these pipes will be below this value, but we estimate that no part inside the tracker will be below -45°C during normal operation.

Without a detailed failure analysis of the future ATLAS cooling system one has to assume the possibility that in the case of a catastrophic failure anywhere in the system the pressure will drop to atmospheric pressure, which will lower the temperature of the coolant to the freezing point of $CO_2$ at -56°C. All components must withstand short-time exposure to this temperature at the maximum allowable pressure.

[2] For a discussion of failure rate estimates see Appendix B.

The maximum temperature for components in the cooling system will be encountered during warm testing of staves during assembly and commissioning. In this case the maximum temperatures in the cooling pipes will be defined by the thermal interlocks, which will cut front-end power if a threshold temperature reached. We estimate that this temperature will not exceed 40°C. This temperature requirement should also cover all cases of external heating of tubes in the tracker.

Any processing temperatures produced (e.g. during welding) should not significantly affect the materials of the circuit (e.g. weaken or cause embrittlement). This includes post-process heat treatments and contact with any specific environment gases during the process.

### 3.6.2 Temperature cycling

Based on the experience from the current SCT operation we expect an average of about 15 cooling system stoppages per year during routine operation. While these do not necessarily lead to a complete warm-up of the system we do require the system to be able to cope with 30 cold-warm cycles per year, or 300 cycles over the anticipated lifetime of the experiment. This includes a safety factor of 2, which also anticipates more frequent stops during the commissioning.

Differently than in the present ATLAS fluorocarbon cooling system the temperature change rate during start-ups of the 2PACL system can be fully controlled. This would not be the case for blow-off systems, which might be used during assembly testing of individual components. Cooling system stoppages will usually involve a gradual warm-up at a rate which is given by the ratio of heat influx and the heat capacity of the system.

Temperature shocks could only occur as the result of fault conditions, in particular a large sudden leak to atmospheric pressure would reduce the temperature to -55°C, the freezing point of $CO_2$.

To conclude we require all components to withstand 300 cycles between 25 and -45°C at a rate of 1°C/s, and 30 cycles instantly from -35°C to -55°C.

### 3.6.3 Radiation

The materials of the components of the cooling circuit must not be adversely affected by the high levels of radiation expected over the lifetime of the HL-LHC. This includes degradation from ionizing radiation as well as neutron fluxes. The materials used must have minimal activation potential from neutron capture. CERN is offering a software package to evaluate the radiological hazards of materials (Actiwiz [8]). Currently this software is restricted to geometries relevant for accelerator geometries, but an extension to typical experiment scenarios is in development

Currently the total ionising dose for the position of the innermost barrel strip layer is forecast at 400 kGray over the expected lifetime of the phase II upgrade years (3000 $fb^{-1}$) [9]. The limit for the 1 MeV neutron equivalent fluence for the same position and for the same period is approximately 1016 $n/cm^2$. Both these values include a safety factor of two. For irradiation effects and verification of activation predictions suitable irradiation testing is required.

## 3.7 Material properties

### 3.7.1 Galvanic properties

Corrosion prevention by design involves the selection of materials to minimise environmental corrosion. We apply this methodology to the cooling system design to avoid poor material interaction with the environment and mating components. The ITk cooling system will inevitably use different kinds of metals in tubes and piping (for example, copper and iron based metals) and galvanic corrosion will contribute to accelerated corrosion of parts of the system unless it is carefully designed.

The materials of the components of the cooling circuit must not be affected by ambient conditions during assembly, transport and integration (rel. humidity up to 80% and temperature up to 25°) and during final operation (50% and -45°C), general chemical exposure (including chosen cooling fluid in radiation environment) or by combination with mating materials.

Corrosion resistance of materials is defined by the galvanic series (or electro-potential series) which determines the nobility of metals. When two metals are submerged in an electrolyte, while electrically connected, the less noble (base) will experience galvanic corrosion. The rate of corrosion is determined by the electrolyte and the difference in nobility. The difference can therefore be measured as a difference in voltage potential.

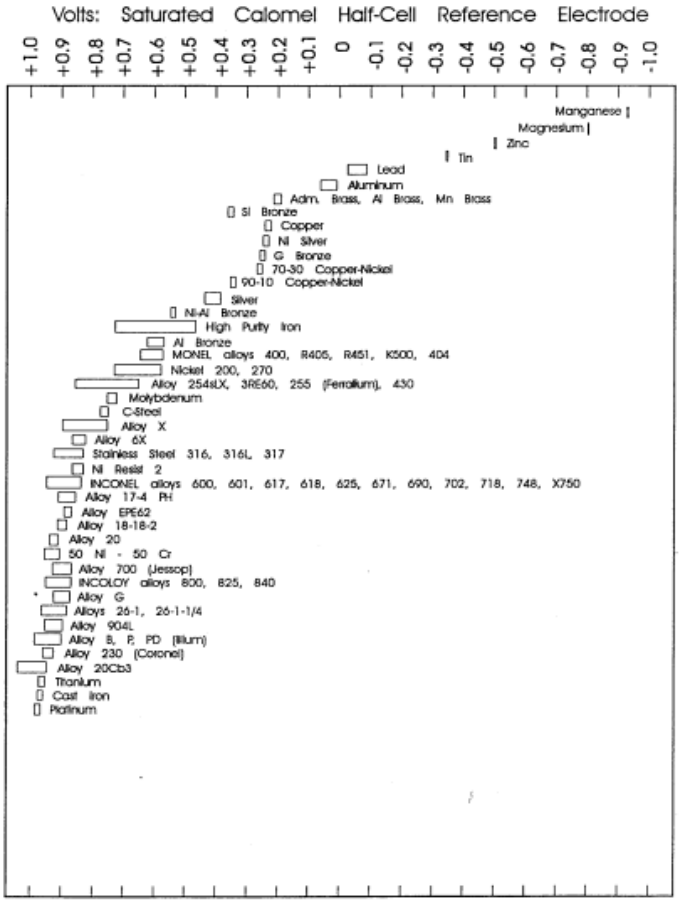


Figure 6: Galvanic series [].

Dissimilar metals and alloys selected for use in the cooling system have different electrode potentials. It is essential through careful design to avoid two or more coming into contact in an electrolyte with one metal acting as anode and the other as cathode. The electro-potential

difference between the dissimilar metals is the driving force for an accelerated attack on the anode member of the galvanic couple. The electrolyte provides a means for ion migration whereby metallic ions move from the anode to the cathode within the metal. This leads to the metal at the anode corroding more quickly than it otherwise would and corrosion at the cathode being inhibited. The presence of an electrolyte and an electrical conducting path between the metals is essential for galvanic corrosion to occur.

Acidity or alkalinity (pH) is also a major consideration with regard to closed loop bimetallic circulating systems. Corrosion inhibition solutions and the use of sacrificial anodes and cathodes is not an option, as they would need to be applied within the plumbing of the system and, over time, would corrode and release particles that could cause potential mechanical damage to circulating pumps, heat exchangers, etc.

Arrangements must be made that during assembly, testing, transport and final operation these environmental constraints are maintained and that exposure to liquid water (condensation) of components destined for installation in the final system is prevented on their inside and outside. In case components are inadvertently exposed to liquid water before installation they should only be used after careful study of the corrosion damage.

### 3.7.2 Other corrosion mechanisms

### 3.7.3 Magnetic properties

The materials of the cooling system should not be significantly magnetic, therefore preventing significant forces on the sub-detector or affecting the path of the particles in the magnetic field. It is therefore preferential to select materials which are non-magnetic. The use of slightly magnetic materials can be considered after assessment of their effects by calculation.

In order to estimate the effect that the pipes will have on the magnetic field we consider two extreme cases. First we calculate the change to the average magnetic field that arises if this magnetic material is distributed uniformly through the volume of the barrel strip tracker. Second we calculate the difference in the integrated curvature of a track which passes through a pipe wall compared with a track which just misses the same pipe.

If pieces of a magnetic material with relative permeability $\mu$, or susceptibility $\chi = \mu$-1, are distributed randomly through a volume, occupying a fraction $f$ of the space, then the effective permeability of the volume becomes $\mu_{eff} = 1 + f\chi$. This applies independently of the shape of the pieces provided both $f$ and $\chi$ are small. If we had an electromagnet with an air gap and we filled the gap with a material with this $\mu_{eff}$ value then the field in the gap would scale with this value. For a material and geometry to be acceptable we require $\mu_{eff}$ to be below $1 + 10^{-4}$, making it negligible compared with other uncertainties of the magnetic field.

For a complete assessment of the effects of magnetic materials in ATLAS we would need to take into account similar contributions from all ITk systems. Here we make the assumption that all the other detectors will be using small amounts of slightly magnetic material similar to the pipes in the barrel strip tracker, which need to satisfy similar requirements.

The pipes are mostly aligned parallel to the magnetic field and this means that the field in the pipe wall is a factor $\mu$ higher than the field just outside. The greatest possible track length in a pipe wall is

the chord which just clips the inner diameter of the pipe, which is approximately 1mm long, while the whole track length in the ITk is approximately 1 m. Thus the fractional difference of $\int Bdl$ between two tracks, one of which just misses and another which just hits a cooling pipe is $(1-\mu)\times10^{-3}$. This difference should be below $10^{-3}$, making it negligible compared with the ultimate momentum resolution of the tracker (1.3%).

The type I tubes in the service gap form a more localized layer of tubes in front of the strip ECs, but without more detailed calculations we assume that the magnetic properties of the type I tubes should be constrained in a similar way as the tubes within the barrel volume.

### 3.7.4 Joinability

We do foresee the need of welded and brazed joints between tubes inside the ID. We therefore require a material choice for the tube material which is compatible with reliable orbital TIG welding and vacuum brazing.

### 3.7.5 Fire Safety

Even in bulk the components of the cooling system are unlikely to generate a significant mass of flammable material. Irrespective of this as the components are in the experimental area they have to comply with relevant CERN regulations [10] in relation to any potentially flammable materials used (for example valves and seals in compressors). A rough assessment of the suitability for use can be made by referring to the halogen content based on manufacturer's specifications; a halogen content of zero or close to is ideal.

## 3.8 Mechanical loads

We expect the cooling system within the inner tracker to be subject to a number of specific mechanical loads:

1. Mechanical stresses induced by the thermal contraction of stave due to the evaporating coolant in the tube and heat on the surface of the stave from the modules. As the stave is large in cross section, has a high modulus and a much lower CTE than the tube the tube will have its length constrained close to its free length as it cools. This will induce mostly axial stresses in the tube.
2. The type I cooling services located in the service gap are also cooled and shrink due to their non-zero CTE. This pulls the pipes that enter the stave out in radius which exerts a bending moment on the tubes themselves and the stave core.
3. As the stave is inserted and serviced forces will be exerted on the tubes. The most significant load planned for is the possibility that the orbital weld head will be hung from the tubes it is joining. After investigation we may conclude that this has to be mitigated by some additional support.
4. We do not expect pulsed pressure forces from the cooling plant; pressure changes will be gradual (tens of seconds). This is partially down to the intended mode of operation, but is also supported by the fact that the system has a high flow resistance and long lines limiting the maximum rate of change of pressure of the bi-phase fluid.
5. We do not expect the magnetic field to oscillate creating Eddie currents, so we do not expect to see induced stresses related to this. The ATLAS magnets could quench, and this

would induce Eddie currents, but this will happen slowly (limited by magnet design) enough to not be of concern.

The first three points in this list will be discussed in detail for our choice of tube material and dimensions in section 4.6.2.

## 3.9 Bend deformation requirements

We require all bends to have no visible local deformations (ripples etc.). Reasonably limited local changes in the cross-section will only have minor effects on pressure drops, we therefore set a requirement of maximum reduction of the cross-section in the bend to 5%. This is achieved for a reduction of one diameter by about 20%, while maintaining elliptical circumference. The reduction of the wall thickness as result of the bending needs to be included in its specification.

## 3.10 On-detector cooling tube requirements

### 3.10.1 Multiple scattering material

While material minimization is always a key requirement for the design of the tracker and its support structure the detailed allocation of the material to different components of the tracker is notoriously badly defined.

The multiple scattering material goal for the ATLAS strip system in the barrel is 2.8% $X_0$ per layer, with 1.8% $X_0$ expected to be taken by the stave including modules [5]. The material of the stave core (incl. tapes) is expected to be around 0.66% $X_0$, of which 0.088% $X_0$ (13.3% of the stave core material) is taken by the cooling tube.

### 3.10.2 Pressure drop

The inner tube diameter is defined by the acceptable pressure drop in the cooling system, which is driven by the acceptable temperature drop. The allocation for the temperature drop on the detector (to the connection points with the type I services) is 3°C, which corresponds to a pressure drop of 1.27 bar at -35°C (including the momentum pressure drop due to the evaporation of coolant corresponding to the nominal heat load on the stave of 140 W).

## 3.11 Geometrical constraints for the on-detector cooling tube

While these do not constitute strict requirements we list here for completeness constraints to the cooling pipe geometry originating from the design of the stave.

### 3.11.5 Tube length

The exact length of the on-detector cooling pipe depends on the options for the on-detector tube shape and the location of the electrical breaks, which are the end points of this tube. The approximate lengths for different geometry options are summarized in Table 1.

**Table 1: Approximate tube lengths for different geometry options.**

| | Electrical break | |
|---|---|---|
| | At end of stave | In service gap |
| Straight 'U' pipe | 2.5m | 2.7m |

| | | |
|---|---|---|
| Additional 'U' for EOS | 2.8m | 3.1m |

### 3.11.6 Bend radii

The centreline bend radii in the current stave geometry are all 15 mm.

## 3.12 Type I cooling pipe requirements

### 3.12.5 Multiple scattering material

The section of the type I pipes where the cooling pipe material is relevant is in the service gap between the barrel and the endcap. It should be noted that the common feed and return lines are not critical in terms of material as they are outside the acceptance of the tracker.

### 3.12.6 Pressure drop

The type I and II return pipes together have to satisfy a similar pressure or equivalent temperature requirement as the on-detector cooling tube. The equivalent temperature drop from the stave end to PP2 needs to be again 3°C or less, which corresponds to a pressure drop of 1.17 bar at -38°C. The material-critical section of the type I pipe is the individual pipe from the stave to the internal manifold, which is in front of the ECs, and therefore should be as small as possible.

For the feed pipes there is only a weak pressure drop constraint. Ultimately, the pressure drop in the complete circuit needs to be within the pressure head provided by the pumps. However, in each manifold branch there needs to be a section with high impedance, to guarantee sufficient flow through all the branches under each evaporator load condition. To achieve this restriction we plan to use a capillary, because the impedance can be well controlled by adjusting the length of the capillary. We require this capillary section to have ten times the flow impedance of the rest of the branch under nominal load, i.e. about 12.7 bar.

## 3.13 Geometrical constraints for the type I cooling tubes

### 3.13.5 Tube length

The type I cooling tubes will consist of two sections: a small diameter section from the stave to an internal manifold within the service module and from there a common section to PP1 at the end of the service module. On the input side the internal manifold will be close to PP1, to allow for a maximum length of capillary before each stave. On the return side the manifold will be as close as possible to the detector to keep the length of the individual return lines short, to allow for the smallest possible dimensions of the tube in the service gap, where material before the endcaps is critical. A detailed discussion of the length of the tube sections is discussed in ref. [2]. Here we do list the maximum tube lengths of each type in Table 2. As can be seen all tube sections in the type I services are shorter than the stave evaporator tube.

**Table 2: Maximum tube length required for the type I services.**

| | Feed | Return |
|---|---|---|
| Individual lines | 2.16m (capillary) | 0.85m |
| Common lines | 0.2m | 1.54m |

### 3.13.6 Bend radii

In the design of the type I cooling tubes in the service gap there are a number of bends required to provide stress relief and allow for access with an orbital TIG weld head. Currently we require bends down to a radius of 8 mm, but this could be increased if there are problems achieving this bend radius.

## 3.14 Electrical breaks

To satisfy the grounding and shielding requirements for the future tracker [] each on-detector cooling pipe needs to be electrically isolated from the others. Consequently, there needs to be an electrical break in each type I pipe (feed and return) between the end of the stave and the internal manifolds. Pipes between the stave end and the break need to be electrically insulated.

A further break is required outside the tracker close to PP1, but is not the subject of this document.

These electrical breaks will need to satisfy the same requirements as outlined throughout this section.

# 4 Cooling Tube Specifications

## 4.1 Material choice

We have investigated the use of a range of different cooling tube materials before focussing on stainless steel (316L) and Titanium (commercially pure grade 2 – CP2). A summary of the most important properties of the candidate alloys is given in Table 3. In this table we list yield strength and ultimate tensile strength figures for fully annealed material, as we anticipate the use of welded or brazed tube joints. These techniques effectively represent an uncontrolled heat treatment of the tubes resulting in an uncontrolled temper around the joint making the use of the properties for fully annealed material the prudent worst case choice[3]. The figure of merit given in the table for each material is a comparison figure intended for the evaluation of materials for the use in particle physics trackers. As is apparent from this number, a Titanium pipe with wall derived from the material yield would have slightly less than half the radiation length of a stainless steel pipe with a similar diameter and its wall thickness specified in the same way.

This table does not attempt to capture the subjective aspects of material description such as weldability or corrosion resistance. These (as will be discussed in later sections) were studied in detail for selected materials with our specific application in mind. It should be noted that the calculation of the required wall thickness following EN or ASME standards prescribes the use of lower yield values, which provides the safety factors inherent to these codes (see also Appendix E and F).

**Table 3: Properties of tube materials.**

| | Stainless steel | Titanium | Aluminium | Cu/Ni | Carbon fibre |
|---|---|---|---|---|---|
| Alloy/grade | 316L(1) | CP2 | 5251 | 70/30 | n/a |
| UNS(2) | S316xx | R50400 | A95251 | C71500 | n/a |
| Density [g/cm$^3$] | 8(3) | 4.51(4) | 2.69(5) | 8.94(6) | 1.6-1.9 (typ.) |
| Radiation length ($X_0$) [mm] | 18 | 36 | 89 | 14 | 230-280 (typ.) |
| Heat conductivity [W/Km] | 14.6(7) | 21.0(8) | 134 | 29 | 1 (typ.)(9) |
| CTE [$10^{-6}$ m/m] | 16.5(7) | 8.4(8) | 25 | 16 | ~0 |
| Modulus [GPa] | 193 | 103 | 70 | 150 | High |
| Yield strength (fully annealed)(10) [MPa] | 290 | 276 | 80 | 88 | n/a |
| Yield strength typical (1/3 hard)(10) [MPa] | 758 | 352 | 190 | 124 | High |
| Ultimate tensile strength [MPa] | 560 | 345 | 180 | 372 | High |
| Figure of merit (Yield)(11) × $X_0$) [$10^6$ kg/s$^2$] | 5.2 | 10.0 | 7.1 | 1.2 | n/a |

*(1) Including derived alloys (316LV, 316LN, etc.)*
*(2) Unified Numbering System for Metals and Alloys*
*(3) http://www.matweb.com/search/DataSheet.aspx?MatGUID=1336be6d0c594b55afb5ca8bf1f3e042&ckck=1 using annealed sheet data. Very close to 316LV or 316LN properties*
*(4) http://www.smithmetal.com/downloads/CPGrade2_SMC.pdf*
*(5) http://www.matweb.com/search/DataSheet.aspx?MatGUID=16bb703f31d6429a95216564dbf857d5*
*(6) http://www.matweb.com/search/DataSheet.aspx?MatGUID=1de470e1f95c442990e87658c7b6eb36*
*(7) between 20°C and 100°C*
*(8) average between -100°C and 0°C*
*(9) perpendicular to fibres*
*(10) 0.2% proof stress*
*(11) using fully annealed yield*

The prime focus in our R&D was on stainless steel and Titanium alloys. Stainless steel is widely used as a tube material and its use and joining techniques are well documented, albeit not commonly for

[3] This is also the approach suggested in ANSI and ISO standards (EN13480 (and PD5500) and ASME boiler and pressure vessel code).

the small, very thin wall tubes in our application. The use of Titanium and its alloys is attractive due to their high strength, low density and large radiation length, and its outstanding corrosion resistance. Titanium can be used from -180°C up to 600°C without loss of toughness whilst resisting creep and oxidisation. Commercially Pure Grade 2 (CP2) Titanium (ASTM Grade 2) has been the focus of our research within the group of Titanium alloys due to its high strength and the fact that it can be seamlessly drawn into tubes and offers excellent weldability. Compared to stainless steel CP2 Titanium has a radiation length twice as large, while the yield strength is very similar.

We also considered Aluminium alloys (e.g. 5251-O), which also have a better figure of merit than stainless steel. However, the low position of Aluminium on the galvanic table makes it challenging to control corrosion[4], and experience [] has shown that there is a high risk of failure. The ATLAS strip upgrade collaboration has therefore decided not to pursue this technology.

In the ATLAS SCT Cu/Ni 70/30 has been used for the on-detector evaporator tubes with an OD of 4.2 mm and an aggressively low wall thickness of 70 µm (working pressure 16 $bar_a$, proof pressure 24 $bar_a$). This material has a thermal conductivity of 29 W/Km, which compares badly with Aluminium alloys, but is better than for Titanium or stainless steels. For the ATLAS application the mechanical properties of 70/30 alloy were entirely adequate. However Cu/Ni has a short radiation length for its modulus and yield strength making this a high material solution compared to other metals.

Cu/Ni 70/30 is primarily marketed for its corrosion resistance in marine applications, which is not a prime consideration for particle physics applications. Because of this specialism, the material is not widely available in the range of sizes and conditions that more common alloys are. For the same reason, there is not the wide technical knowledge base for joining and heat treatment, or support from manufacturers that exists for titanium or aluminium alloys. It can be welded, brazed and soft soldered. However, welding and brazing are difficult and specialised and the joints show susceptibility to stress-corrosion cracking.

One problem encountered during the pre-production of cooling pipes for the ATLAS SCT was that the Cu/Ni 70/30 alloy in fully annealed condition had a large and open grain structure with respect to the 70 µm wall thickness. This left the material susceptible to grain boundary defects across the entire wall, which resulted in leaks which were difficult to identify. Ultimately this was solved by careful attention to post-annealing grain refinement, so that no problems were encountered during the manufacture and operation of this system.

In our R&D for the ATLAS upgrade we did not pursue cupro-nickel alloy because of its poor figure of merit, and the challenges it presents for welding and brazing.

Carbon fibre would be an attractive material choice for its large radiation length and the matching thermal expansion properties to the CF support structures. However, we did not pursue this technology further because of the typically poor cross-wall heat conductivity and the high stiffness, which compared to the compliance displayed by metallic tubes makes their integration into the detector more difficult. Also, joining CF tubes reliably is challenging and experience has shown that

[4] Primarily its separation in galvanic potential from all the other possible pipe materials such as stainless steel that will inevitably be within the cooling system.

liquid $CO_2$ can dissolve the cyanate ester resin in the composite. The use of CF tubes has been investigated for the IBL, but results have not been published. However, a description of these studies can be found at [11].

## 4.2 Temper

Temper is a term usually associated with carbon steel to describe the crystalline structure of the steel and its associated properties. In the context of this document we are studying a number of non-ferrous materials, and whilst the term 'temper' is something of a misnomer we will use it to discuss the available yield and ultimate tensile strength properties available in a material through heat treatment.

All the metallic candidate materials have their lowest yield strength when they are fully annealed. This yield strength rises as the temper is increased all the way up to fully hard. Depending on the material the ultimate tensile strength is also likely to rise, and the yield strength and the ultimate tensile strength will converge.

As already introduced in section 4.1 we use the properties of fully annealed material for our tube specifications. This is because of the effects of joining techniques, which raise the temperature of the tubes, like welding or brazing.

The weld process causes the formation of a molten pool of metal that cools in an uncontrolled manner. This causes a local area of the material to have a different and unknown temper. Both ISO and ANSI standards stipulate that fully annealed material properties should be assumed when taking the yield strength to calculate the maximum permissible pressure. This approach is conservative and prevents concerns with the catastrophic failures that can occur if a material is pushed above its ultimate tensile strength.

Depending on the choice of material it might appear that there is considerable scope to use the material more efficiently. To do this one would use the yield properties for half, or fully hard material for the dimensioning of the tube walls. This would allow for thinner walls and thus lower material. This approach is especially appealing with some Titanium alloys where the temper has a huge influence over the yield (factor of more than 2). Whilst this argument is logical there are two significant drawbacks in its use:

1. For materials with a large change in yield due to temper there is a tendency for the Ultimate Tensile Strength (UTS) to end very close to the yield, this makes using high yield values dangerous as at the fault loads the structure would be perilously close to catastrophic failure.
2. All the standards that describe best practice support using the fully annealed yield values and whilst the standards might not be directly applicable to our application contradicting one of their principal recommendations would need a lot of research and justification.

Further to the consequences for the dimensioning of the tube wall the tube temper needs to be considered for bending. A fully hard pipe will be much more difficult to bend than a fully annealed one. It is possible that either the outer wall will exceed the ultimate tensile strength and snap, or that the inner wall (in compression) will buckle and ripple during the bending process, requiring an increase in bend radius.

We specify bright annealed soft temper for stainless tubes.

## 4.3 Magnetic properties

Among the options considered for the pipe material Aluminium, Carbon and Titanium are effectively non-magnetic. The only option that we have to consider further is the 316L stainless steel. This is an austenitic steel and austenite itself is non-magnetic. On cooling to room temperature austenite tends to rearrange to the martensite structure which is ferromagnetic. However this tendency is blocked in the 300 series by the presence of nickel. The magnetic permeability of annealed 316L is typically in the range 1.002 to 1.005. The permeability of 300 series stainless can be increased by cold-working. Generally speaking, the higher the nickel content the more stable the austenitic structure and less magnetic response from cold-working. Consequently 316 stainless steel, with higher amounts of nickel, exhibits virtually no magnetism after cold-working in most cases. While 304, with lower nickel content, may become mildly magnetic. We make the assumption that the stave cooling pipes would start with annealed 316L and the amount of cold-working involved in their construction would not significantly change their properties so a permeability value of 1.005 is conservative.

To estimate the effective permeability for uniform material distribution we assume $\chi = 1.005$ and a barrel strip tracker volume of 7 $m^3$. The estimated pipe volume in the barrel strip volume is $V \approx 500$ staves × 2.53 m × ((2.25 mm)$^2$ – (2 mm)$^2$) × $\pi/4 = 10^{-3}$ $m^3$. So $\mu_{eff} = 1 + 7\times10^{-7}$, which is acceptable. We estimate the variation of the magnetic field integral for 316L stainless steel to be $5\times10^{-6}$ which is deemed to be negligible.

The assumed value for the permeability of stainless steel (1.005) should be verified once pre-production prototypes of the tubing become available.

## 4.4 Tube manufacturing

### 4.4.1 Drawing process

### 4.4.2 Tube length constraints

REACH regulations limit the size of chemical baths used in the preparation of the cooling tubes. Practically this limits the tube length from our suppliers to 3.2 m; longer tube lengths would require a significant additional investment.

### 4.4.3 Tube diameter constraints

Minimum tube diameters which are commercially available for stainless steel or titanium are significantly smaller than our requirements (Ti CP2 ID 0.380mm, OD 0.595mm).

## 4.5 Tube diameter choices

Semi-empirical models [12] can be used to predict the pressure drop for a straight tube of given diameter (Table 4). It should be noted that these models are known to have limited accuracy, especially as they do not take into account geometrical factors like bends, and as our application is outside of the range of parameters for which many of these models have been developed. We have therefore tested the predictions of these models with realistic stave cooling tube prototypes [2].

Our calculations have been done using two different programs, which both use similar underlying two-phase flow models. In each program the length of the tube is divided into small sections and the changes of pressure and enthalpy are calculated based on the state of the coolant in this section. Both programs use the flow-pattern-based frictional pressure drop and heat transfer models developed by Thome et al., specifically for the use with $CO_2$ [13]. In addition, one of the two programmes (FLUDY) also allows the use of other models for cross-check, of which we use the model by Friedel [14] for the pressure drop predictions, and by Chen [15] for the heat transfer. It should be noted that the pressure drops predicted by these methods are lower than the Thome model, whereas the heat transfer predictions are comparable (for the same heat flux into the coolant).

The expected tube geometries in the future inner tracker, and in particular the lengths of individual sections, on which the predictions described here are based, are described in ref. [2].

The results of our calculations for the on-stave evaporators are summarized in Table 4. We list the minimal inner diameters compatible with the temperature drop requirements outlined in section 3.10.2 ($\Delta T \leq 3°C$), as well as the temperatures for an inner diameter of 2mm. This diameter has been chosen based on original estimates for the stave power and we have developed the orbital TIG welding techniques required for such small tubes. Calculations using revised power estimates suggest that smaller diameters could be possible, but our experience shows that it will be hard to use orbital TIG welding for diameters below 2 mm and keeping the original dimension gives us a margin if the predictions of the models are significantly off. Reducing the diameter from this value to 1.77 mm would save about 20% of the cooling pipe material, but as noted, significantly increase the challenges associated with joining.

**Table 4: Coolant temperature and HTC predictions for the on-detector cooling tube using different models for 2-phase flow ($P_{stave}$ = 140 W, $mf$ = 1g/s, $l$ = 2.52 m, $x_{in}$ = 0, heat load distributed evenly along pipe). For methods see references in the text.**

| Program | Method | | ID [mm] | $T_{start}$ [°C] | $T_{end}$ [°C] | $\Delta T$ [°C] | $HTC_{start}$ [kW/Km] | $HTC_{end}$ [kW/Km] |
|---|---|---|---|---|---|---|---|---|
| | $\Delta p_{frict}$ | HTC | | | | | | |
| FLUDY | Thome | | 1.77 | -35 | -38 | 3 | 4.9 | 13.1 |
| | Thome | | 2 | -35 | -36.5 | 1.5 | 4.5 | 10.4 |
| | Thome | Chen | 1.77 | -35 | -38 | 3 | 4.8 | 11.9 |
| | Friedel | Chen | 1.42 | -35 | -38 | 3 | 5.6 | 14.9 |
| | Friedel | Chen | 2 | -35 | -35.7 | 0.7 | 4.4 | 9.6 |
| COBRA | | | | | | | | |

Table 5 lists the results of similar calculations for the type I services up to PP1. The parameters used (tube section lengths, mass flows) are worst case estimates, and do not apply to most of the circuits. The pressure drop calculations include a hydrostatic pressure drop due to a maximum difference in radius of ~60 cm for a pure liquid column (0.06bar), which only applies for a fraction of the circuits. The pressure drop in the type I section is dominated by the individual sections, which have an aggressively small diameter to minimize the material in the service gap. Again, it should be noted that the calculations do not take bends into account and must be verified in realistic prototype setups, all the more as the smallest diameter tubes are buried deep inside the strip tracker and cannot be changed once the barrel strip system is built.

Assuming that the type II return pipes have the same inner diameter as the common type I pipes (5.75 mm) and even if we assume that they will be 10 m long (twice the difference in radius from the

beampipe between PP1 and PP2), the pressure drop in the type II pipes will be dominated by the hydrostatic pressure drop (~0.55 bar for 5 m liquid column at -40°C), and we expect a maximum equivalent temperature drop of about 1.2°C in these lines. This means that from these predictions the goal of a total equivalent pressure drop in the type I and type II services of 3°C (see section 3.12.6) can be achieved with the proposed geometries.

**Table 5: Pressure drops and equivalent temperature gradients for the type I tube using different models for 2-phase flow ($x$ = 0.5, $T_{stave,out}$ = -38°C) for the individual ($mf$ = 1 g/s, $l$ = 1.43 m) and common ($mf$ = 2 g/s, $l$ = 1.64 m) type I tube sections. For methods see references in the text.**

| Program | Method | Individual section | | | Common section | | |
|---|---|---|---|---|---|---|---|
| | | ID [mm] | $\Delta p$ [bar] | $\Delta T$ [°C] | ID [mm] | $\Delta p$ [bar] | $\Delta T$ [°C] |
| FLUDY | Thome | 2.1 | 0.81 | 2.0 | 5.45 | 0.01 | 0.03 |
| | Friedel | 2.1 | 0.29 | 0.8 | 5.45 | 0.01 | 0.01 |
| COBRA | | | | | | | |

The choice of inner diameter for the capillaries will be a compromise between the length of capillary required to achieve the required pressure drop (~12 bar), and the risk of blockage for very small diameters. At present we intend to use capillary with an inner diameter of 500 µm, because this dimension was readily available from commercial suppliers. This choice will be verified with prototype tests (see ref. [2]).

## 4.6 Wall thickness choices

### 4.6.1 Design by Formula

For the calculation of the required wall thickness standardized formulas are available. However, it should be noted that these formulas have been developed for unconstrained tubes. The stave cooling loop tube is glued into foam channels within the stave core and is therefore not free. A simple calculation for free tubes will not be correct because of longitudinal stress modes experienced by the tube due to this constraint. Nevertheless we use design by formula for a first estimate of the wall thickness, which we then verify by design FE Analysis (see section 0).

Material values are a key input to these calculations. As justified above (section 4.2) we will be working with the conservative assumption of a fully annealed tube. In addition we will use 'book' material values from the EN and ANSI standards. Note that these fully annealed book values may vary from the figures in Table 3. Possible variations are discussed where applicable.

#### *4.6.1.1 Wall thickness for on-stave evaporator in stainless steel*

For stainless steel we base our calculations of the tube wall thickness on EN 13480. This standard focuses primarily on steel piping with a small subsection for aluminium alloys but it does not cover any other tube materials. A detailed discussion of the calculations and its inputs is given in Appendix E. The results of these calculations are listed in Table 6.

**Table 6: Tube wall dimensions for stainless steel 316L calculated according to EN13480 (for maximum allowable pressure of 130 $bar_g$, joint coefficient 1, maximum allowable stress 150 MPa).**

| $D_o$ [mm] | $e$ [mm] | $e_{bend}$ [mm] |
|---|---|---|
| 2.275 | 0.103 | 0.107 |
| 3.175 | 0.144 | 0.151 |

#### 4.6.1.2 Wall thickness for on-stave evaporator in titanium

Titanium pipe is not referenced at all in the EN standards. However, the ASME Boiler and Pressure Vessel code does reference Titanium and how to work with it. We have used the procedures outlined in this document (discussed in detail in Appendix F). The resulting wall thickness for different tube diameters are listed in Table 7.

**Table 7: Minimum wall thickness for CP2 Titanium tubes according to the ASME Boiler and Pressure Vessel code (maximum allowable working pressure 130 $bar_a$, longitudinal joint efficiency 1, and maximum allowable stress 86.1 MPa).**

| OD [mm] | Wall thickness [mm] |
|---|---|
| 2.275 | 0.162 |
| 3.175 | 0.226 |

For these dimensions the cross-sectional area for tubes with the same outer diameter is larger by about 50% for titanium than for stainless steel. The radiation length for stainless steel is double the one for titanium, so that the multiple scattering material of titanium pipes is smaller by 25% than for stainless steel.

Currently we foresee to use a 2.275 mm OD titanium tube with 160µm wall thickness for the stave cooling tube.

As reported in ref. [2] we have demonstrated orbital TIG welding for tubes with 2.275 mm OD down to wall thicknesses of 120 µm. According to the ASME BPV code the maximum allowable working pressure for such a tube would be 95 $bar_g$.

#### 4.6.1.3 Calculations for type I tubing

In a similar fashion than for the on-stave evaporator tubes we have also calculated the minimum wall thickness for the type I tube dimensions (Table 8).

**Table 8: Minimum wall thickness for type I transfer pipes for stainless steel (as derived from EN 13480) and titanium (from ASME BPV code).**

| | Minimum wall thickness [mm] | |
|---|---|---|
| OD [mm] | For stainless steel 316L (according to EN 13480) | For titanium (according to ASME BPV) |
| 2.5 | 0.117 | 0.178 |
| 3.175 | 0.151 | 0.234 |
| 6.35 | 0.313 | 0.452 |

We plan to use titanium tubes with 2.5 mm OD and 200 µm wall thickness for the individual return lines, and tubes with 6.35 mm OD and 450 µm wall thickness and 3.175 mm OD and 250 µm wall thickness for the common return and feed lines, respectively. It should be noted that the common feed and return lines are not critical in terms of material as they are outside the acceptance of the tracker. The individual feed lines will be titanium capillaries, for which the wall thickness (500 µm) is defined by manufacturing constraints, with a strength well above our pressure requirements.

### 4.6.2 Design by analysis

As noted in the section 4.6.1 designing by standard and formula is only appropriate for a limited number of scenarios. In loading conditions outside these scenarios the hand calculations either need to be extended or FEA solutions investigated, or both.

The situations within the tracker upgrade that require further investigation are:

1. Forces on the staves with the isolation provided by the compliance of the stave tails.
2. The stresses in the pipes as the radial type I services expand and contract due to thermal effects.
3. The fully encapsulated pipe within the stave.

These areas have been studied in turn.

#### *4.6.2.1 Forces on the staves with the isolation provided by the compliance of the stave tails, both within the tails and the radial services (1 &2)*

This study built a series of models of the cooling tubes as they emerge from the stave core up to the point where they are supported on the barrel interlinks. The relative position of these tube end points can only be guaranteed within limits and this study aims to understand how much displacement of the tube end is needed to threaten damage to the stave core, and what thermal or mechanical loads would be required to cause these damaging effects.

The pipe immediately outside the stave is modelled, with one end constrained and the other end displaced. This geometry is shown in Figure 7. For titanium pipe with 0.12 mm wall thickness we have reaction forces of 0.7 N and maximum stresses of 44.58 MPa with a 0.25 mm motion of the left hand end.

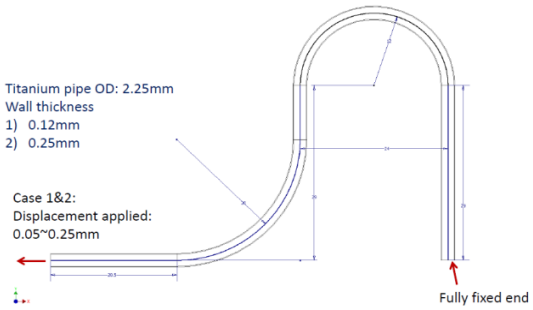


**Figure 7: Geometry of FEA study of stress in the cooling tube between stave and interlink.**

Subsequently the tube is subjected to indicative thermal loads. The results from the displacement study are fed into a second model which applies a thermal load to the Titanium pipe and estimates the pipe end displacement caused by an assumed stave thermal contraction. From this it can be seen that a $\Delta T$ of 60°C might cause the stave to contract 0.252 mm and this would induce a stress of 94.5 MPa in the pipe and a reaction force of 0.8 N.

Note: Stave CTE assumed: ~3.5E-6 ppm

| | | | wall thickness | |
|---|---|---|---|---|
| | Input parameters | | 0.12mm | 0.25mm |
| Time step | Load curve 1 temp °C | Load curve 2 Displacement introduced by stave mm | max stress MPa | max stress MPa |
| 0 | 25 | 0 | 0 | 0 |
| 1 | 15 | -4.20E-02 | 15.755 | 16.495 |
| 2 | 5 | -8.40E-02 | 31.509 | 32.99 |
| 3 | -5 | -0.126 | 47.264 | 49.485 |
| 4 | -15 | -0.168 | 63.019 | 65.981 |
| 5 | -25 | -0.21 | 78.774 | 82.476 |
| 6 | -35 | -0.252 | 94.528 | 98.971 |
| | Reaction force at the fix end N: | | 0.8 | 1.6 |

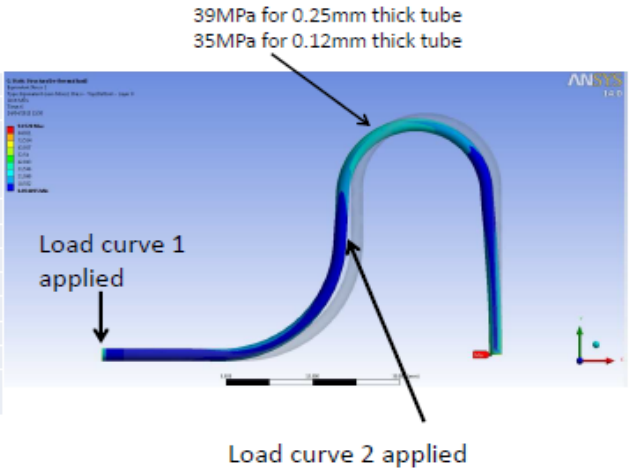


**Figure 8: FEA study of stress in tube between stave and interlink for different stave temperatures.**

This model was then extended to explore the pipe as it goes on out through the services gap (Figure 9). The model above is used as a start point and the results are fed into a new model with a radial pipe. Here it can be seen that the contraction of the radial pipe appears to reduce the pipe stresses – this is because the model has a longer free pipe and so the loads cause smaller displacements.

| | | | wall thickness | |
|---|---|---|---|---|
| input parameters | | | 0.12mm | 0.25mm |
| Load curve 1 temp °C | Load curve 2 displacement in radial dir mm | Load curve 3 displacement at stave end mm | max stress Mpa | max stress Mpa |
| 25 | 0 | 0 | 0 | 0 |
| 15 | 0.0516 | -4.20E-02 | 12.446 | 13.722 |
| 5 | 0.103 | -8.40E-02 | 24.878 | 27.425 |
| -5 | 0.155 | -0.126 | 37.351 | 41.185 |
| -15 | 0.206 | -0.168 | 49.756 | 54.849 |
| -25 | 0.258 | -0.21 | 62.229 | 68.61 |
| -35 | 0.31 | -0.252 | 74.703 | 82.371 |

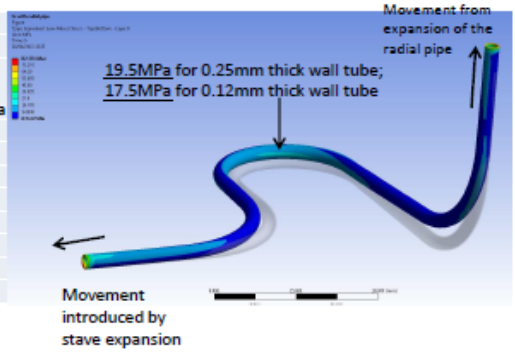


**Figure 9: FEA study of stress in tube between stave and interlink with radial tube section.**

Finally, the model is extended to look at the full length of the tube in the service gap for a stave on barrel 3 (assumes single radial pipe of same dimensions as stave pipe). Again, the inputs are from the earlier studies. Once more the stress falls as the structure is longer and the displacements produce lower strains, and we introduce just 10 MPa stress onto the system.

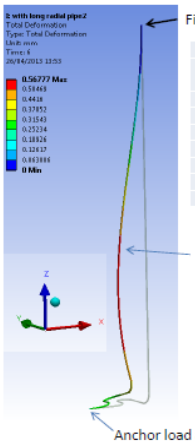


| Input parameters | |
|---|---|
| temp °C | Anchor load displacement mm |
| 25 | 0 |
| 15 | -4.20E-02 |
| 5 | -8.40E-02 |
| -5 | -0.126 |
| -15 | -0.168 |
| -25 | -0.21 |
| -35 | -0.252 |

Max stress on both 0.12 mm and 0.25mm wall thick tubes are very small (well below 10MPa).

Max displacement (X-dir) = -0.37mm
Max displacement (Y-dir) = 0.37mm;
**Max displacement (Z-dir) = 0.31mm**

Figure 10: FEA study of stress in tube between stave and interlink with full-length radial tube section.

From this series of studies we conclude that these stresses are low enough that we are not concerned about them until the pipe geometry and dimensions are finalised. Once this is done we will revisit these studies and verify that the pipe stresses are not problematic.

#### *4.6.2.2 Stress in the fully encapsulated tube within the stave*

The cooling tube is glued into carbon foam blocks over the full length within the stave core and is therefore fully encapsulated within the stave. This can introduce complex forces when the pipe is loaded. The two specific areas of concern are loading due to internal pressure and the thermo-mechanical loading when the stave is cooled. Both these loads will occur together in operation.

At present (autumn 2014), we have done some work in this area but have not yet collected sufficient evidence to demonstrate with FEA what our margins of safety are. However, it should be noted that of ten full size prototypes we are yet to experience any problems.

The problem is best described by bounding it:

- A full 1.3m long pipe would contract 694microns in its free state, when constrained at either end. This would result in a stress of 56MPa and a contraction force of 64kN (cross section = 1.14mm (2.275OD x 0.16WT))
- If the stave core is rigidly bonded to the pipes it will have to withstand the force above. If the entire load is carried on the two skins a contraction of 0.25mm might be expected.
- However, if the core shears the contraction of the core will be less and the pipe will contract more and both will contain lower stresses (but the shearing layer will be more highly stressed).

To date we do not have a convincing model of how the movements and stresses are distributed within the stave. We need to do more work in this area combining both experimentation and FEA and establish what the pipe and stave core stresses are to ensure we are using appropriate safety factors.

### 4.6.3 Joining considerations

### 4.6.4 Handling considerations

## 4.7 Surface treatment (pickling)

## 4.8 Other tube specifications

- Tube tolerances: Tolerance on the OD will be ±0.05mm (including ovality). Tolerance on wall thickness will be 0/+0.02mm (including eccentricity).
- Surface Finish: ID surface finish of 0.8µm (1.6µm may be accepted if 0.8µm is unlikely to be achieved). OD surface finish of 0.8µm
- Defects: A permissible level of defects is listed in
- Dressing or polishing of scratches or abrasions is not permitted, as this will locally thin the already fine wall of these tubes.

Table 9: Defects on tube surface including acceptance or rejection criteria.

| Type of Defect | Acceptance Criteria |
|---|---|
| Score marks | Allowable defect depth: less than 3% of nominal wall thickness |
| Handling or seizure marks<br>Smears | Allowable defect depth: Less than 3% of wall thickness with a maximum of 1 defect per metre length of tube |
| Extrusion or drawing stoppage and resumption marks<br>Embedded particles<br>Cracks<br>Blisters<br>Superficial corrosion (including pitting or galvanic) | Will be rejected |

- Grain size: Grain size width should not exceed 25% of wall thickness through the cross section of the wall in the final annealed or tempered condition.

- Cleanliness: The tube must be free from contamination such as oils or greases, particulates, or moisture. All tubes must be capped prior to transport. The tubes must not contact water in any stage of manufacturing. If this is impossible due to the manufacturing process a suitable drying method may be required.

## 4.9 Tube QA

All parts of the cooling system need to be designed to work appropriately in the ATLAS ITk environment through the lifetime of the experiment. Once the design is complete we need to make sure that all the delivered parts are to the design and that the design is appropriate.

At this stage of the project the complete procedures have not been defined but the following considerations will be central to the procedures:

- Pipe inspection and testing: The pipe vendor will pressure test the pipes and certify that they pass. We then will fabricate the structures with bends and test fittings and we will need to test them to make sure they have not been damaged. The exact testing procedure and the integration into the stave production and QC sequence will still need to be defined;
- Dimensions of pipes will be verified by batch tests;
- Pressure testing: as outlined in section 3.2, all components need to be pressure tested to 186 $bar_a$.
- Weld qualification: BS EN 13480-4:2012 has a well-documented weld qualification procedure. We intend to follow this or another comparable standard;
- Weld inspection: As well as qualifying the fittings we need to make sure the welds are up to standard. Again this procedure will be developed in line with BS EN 13480-4:2012 and will probably draw heavily on BS EN ISO 15614-1:2004+A2:2012;
- Fitting qualification:
- Fitting inspection:

## 4.10 Handling and storage

Whilst the principal design requirements of these tubes should ensure that their performance is not reduced in normal usage it is prudent to look after them before they are commissioned. With this in

mind the following handling and storage requirements are suggested. It should be noted that failure to do this may not link to a failed product, but the measures are sufficiently easy and prevent damage that could be catastrophic.

- The raw pipe should be stored in a non-condensing atmosphere in a non-conductive container. If this is done the atmosphere can be air as there is no real way the moisture in the atmosphere can behave as an electrolyte promoting corrosion.

# Appendix A: ATLAS barrel strip stave power estimates

The power estimate for a barrel strip stave has been evolving throughout the project as the components on the stave and the designs have become more and more developed and refined, and realistic prototypes have become available. Because of the better knowledge of the system safety factors used in past estimates can now be reduced.

The first estimates were documented in the original cooling system requirement document [4]. This document used safety factors of ×1.1 to allow for changes of size and segmentation, and ×1.25 to account for uncertainties in the electronics power estimates because the front-end electronics were in the early stages of design. The stave power for a short-strip stave in this document is 142 W/stave (nominal, at start-up) and 230 W/stave (incl. safety factors, after irradiation). The latter number includes 36 W of leakage power, which has been estimated for $\int L = 6000\ fb^{-1}$ (twice nominal HL-LHC) and includes a safety factor of 2 for the thermal impedance from the sensor to the coolant. This value (230 W) has been used to derive the original tube diameter specifications. The document also gives power estimates for the long-strip staves, which are 44 W (nominal, at start-up) and 68 W (incl. safety factors, after irradiation). However, we do want to arrive at one common stave core design for short- and long-strip staves, and therefore the cooling tube dimensions will be determined by the high power case.

In the LOI [5] and the associated back-up document on stave core design [3] the stave electronics power is estimated as 133 W and 146 W, respectively. The leakage power is not directly estimated, but can be deferred from results in the latter document to be 6 W for the complete stave at a coolant temperature of -35°C. No safety factors are used (except for the leakage power estimated for $\int L = 6000\ fb^{-1}$).

Since these estimates first prototypes of the ABC130 read-out chips have been received. Measurements of the currents required by these chips, and a better understanding of the efficiencies achieved by the stave powering technologies (DC/DC conversion efficiency 77%) allow us to reduce our estimates on the electronics power for a stave to about 100 W. With the better understanding of the future barrel strip system we can also reduce the safety factors and retain only a safety factor of ×1.1 for uncertainties in the electronics power, resulting in a stave electronics power estimate of 110 W.

Finally, we estimate the leakage power after irradiation to be within 30 W (incl. safety factors on thermal impedance and cooling temperature) for the whole stave.

Our current maximum total stave power estimate including safety factors after irradiation is therefore 140 W.

# Appendix B: Properties of $CO_2$

**Table 10: Saturation properties of $CO_2$ [16].**

| Temperature [°C] | Pressure [$bar_a$] | Liquid Density [$kg/m^3$] | Vapour Density [$kg/m^3$] | Liquid Enthalpy [kJ/kg] | Vapour Enthalpy [kJ/kg] | Liquid Entropy [kJ/kgK] | Vapour Entropy [kJ/kgK] |
|---|---|---|---|---|---|---|---|
| -53.115 | 6 | 1166 | 15.839 | 86.796 | 431.65 | 0.55197 | 2.1192 |
| -49.369 | 7 | 1152.2 | 18.372 | 94.191 | 432.87 | 0.5849 | 2.0984 |
| -46.005 | 8 | 1139.6 | 20.908 | 100.87 | 433.86 | 0.61414 | 2.0801 |
| -42.941 | 9 | 1127.9 | 23.452 | 106.99 | 434.65 | 0.64052 | 2.0638 |
| -40.122 | 10 | 1116.9 | 26.006 | 112.66 | 435.3 | 0.6646 | 2.0491 |
| -37.504 | 11 | 1106.5 | 28.572 | 117.95 | 435.81 | 0.68681 | 2.0357 |
| -35.057 | 12 | 1096.7 | 31.153 | 122.93 | 436.22 | 0.70745 | 2.0233 |
| -32.757 | 13 | 1087.2 | 33.752 | 127.65 | 436.54 | 0.72677 | 2.0117 |
| -30.583 | 14 | 1078.2 | 36.368 | 132.13 | 436.77 | 0.74496 | 2.0009 |
| -28.521 | 15 | 1069.5 | 39.005 | 136.41 | 436.93 | 0.76215 | 1.9906 |
| -26.557 | 16 | 1061 | 41.663 | 140.52 | 437.02 | 0.77848 | 1.9809 |
| -24.682 | 17 | 1052.8 | 44.345 | 144.46 | 437.06 | 0.79405 | 1.9716 |
| -22.886 | 18 | 1044.8 | 47.05 | 148.27 | 437.04 | 0.80894 | 1.9628 |
| -21.162 | 19 | 1037 | 49.782 | 151.95 | 436.97 | 0.82321 | 1.9543 |
| -19.503 | 20 | 1029.4 | 52.54 | 155.52 | 436.85 | 0.83694 | 1.9461 |
| -17.903 | 21 | 1021.9 | 55.327 | 158.99 | 436.69 | 0.85018 | 1.9382 |
| -16.359 | 22 | 1014.5 | 58.144 | 162.36 | 436.49 | 0.86296 | 1.9305 |
| -14.864 | 23 | 1007.3 | 60.992 | 165.64 | 436.25 | 0.87533 | 1.923 |
| -13.417 | 24 | 1000.2 | 63.872 | 168.85 | 435.97 | 0.88732 | 1.9158 |
| -12.013 | 25 | 993.2 | 66.786 | 171.98 | 435.66 | 0.89897 | 1.9087 |
| -10.65 | 26 | 986.27 | 69.736 | 175.05 | 435.32 | 0.91031 | 1.9018 |
| -9.3243 | 27 | 979.42 | 72.722 | 178.06 | 434.94 | 0.92134 | 1.895 |
| -8.0342 | 28 | 972.64 | 75.747 | 181.01 | 434.53 | 0.93211 | 1.8884 |
| -6.7775 | 29 | 965.92 | 78.812 | 183.9 | 434.08 | 0.94263 | 1.8818 |
| -5.5521 | 30 | 959.25 | 81.919 | 186.75 | 433.61 | 0.95291 | 1.8754 |
| -4.3564 | 31 | 952.63 | 85.07 | 189.56 | 433.11 | 0.96298 | 1.8691 |
| -3.1886 | 32 | 946.05 | 88.266 | 192.32 | 432.57 | 0.97285 | 1.8628 |
| -2.0474 | 33 | 939.5 | 91.509 | 195.05 | 432.01 | 0.98253 | 1.8566 |
| -0.93132 | 34 | 932.97 | 94.803 | 197.74 | 431.42 | 0.99203 | 1.8505 |
| 0.16082 | 35 | 926.47 | 98.148 | 200.39 | 430.8 | 1.0014 | 1.8444 |
| 1.2302 | 36 | 919.98 | 101.55 | 203.02 | 430.15 | 1.0106 | 1.8384 |
| 2.2778 | 37 | 913.5 | 105 | 205.62 | 429.47 | 1.0196 | 1.8324 |
| 3.3047 | 38 | 907.02 | 108.52 | 208.19 | 428.76 | 1.0286 | 1.8264 |
| 4.3117 | 39 | 900.54 | 112.1 | 210.74 | 428.02 | 1.0374 | 1.8204 |
| 5.2997 | 40 | 894.05 | 115.74 | 213.27 | 427.25 | 1.0461 | 1.8145 |
| 6.2695 | 41 | 887.54 | 119.45 | 215.78 | 426.44 | 1.0547 | 1.8086 |
| 7.2218 | 42 | 881.02 | 123.24 | 218.28 | 425.61 | 1.0632 | 1.8027 |
| 8.1574 | 43 | 874.47 | 127.1 | 220.75 | 424.74 | 1.0716 | 1.7967 |
| 9.0767 | 44 | 867.89 | 131.04 | 223.22 | 423.84 | 1.0799 | 1.7908 |
| 9.9804 | 45 | 861.27 | 135.07 | 225.68 | 422.9 | 1.0882 | 1.7848 |
| 10.869 | 46 | 854.6 | 139.18 | 228.12 | 421.93 | 1.0964 | 1.7788 |
| 11.743 | 47 | 847.88 | 143.4 | 230.56 | 420.92 | 1.1046 | 1.7728 |
| 12.604 | 48 | 841.1 | 147.71 | 233 | 419.88 | 1.1127 | 1.7667 |
| 13.45 | 49 | 834.25 | 152.13 | 235.43 | 418.79 | 1.1208 | 1.7606 |
| 14.284 | 50 | 827.32 | 156.67 | 237.87 | 417.66 | 1.1289 | 1.7544 |
| 15.105 | 51 | 820.3 | 161.34 | 240.3 | 416.48 | 1.1369 | 1.7481 |
| 15.913 | 52 | 813.18 | 166.13 | 242.74 | 415.26 | 1.1449 | 1.7417 |
| 16.71 | 53 | 805.96 | 171.07 | 245.19 | 413.99 | 1.153 | 1.7353 |
| 17.495 | 54 | 798.61 | 176.17 | 247.65 | 412.66 | 1.161 | 1.7287 |
| 18.269 | 55 | 791.13 | 181.43 | 250.13 | 411.28 | 1.1691 | 1.7221 |
| 19.031 | 56 | 783.49 | 186.87 | 252.62 | 409.83 | 1.1772 | 1.7153 |
| 19.783 | 57 | 775.69 | 192.52 | 255.13 | 408.32 | 1.1854 | 1.7083 |
| 20.525 | 58 | 767.69 | 198.39 | 257.67 | 406.73 | 1.1936 | 1.7011 |
| 21.256 | 59 | 759.48 | 204.5 | 260.24 | 405.07 | 1.2019 | 1.6938 |
| 21.978 | 60 | 751.03 | 210.88 | 262.85 | 403.32 | 1.2102 | 1.6862 |
| 22.69 | 61 | 742.31 | 217.57 | 265.49 | 401.47 | 1.2188 | 1.6784 |
| 23.392 | 62 | 733.26 | 224.6 | 268.19 | 399.52 | 1.2274 | 1.6703 |
| 24.084 | 63 | 723.84 | 232.03 | 270.96 | 397.44 | 1.2363 | 1.6618 |
| 24.768 | 64 | 713.99 | 239.91 | 273.79 | 395.22 | 1.2453 | 1.6529 |
| 25.442 | 65 | 703.62 | 248.33 | 276.72 | 392.84 | 1.2547 | 1.6436 |
| 26.108 | 66 | 692.62 | 257.39 | 279.76 | 390.27 | 1.2644 | 1.6336 |
| 26.765 | 67 | 680.85 | 267.23 | 282.95 | 387.47 | 1.2745 | 1.623 |
| 27.413 | 68 | 668.1 | 278.05 | 286.32 | 384.37 | 1.2852 | 1.6115 |
| 28.052 | 69 | 654.08 | 290.16 | 289.93 | 380.9 | 1.2967 | 1.5988 |
| 28.683 | 70 | 638.31 | 304.03 | 293.88 | 376.91 | 1.3093 | 1.5844 |
| 29.304 | 71 | 619.92 | 320.56 | 298.35 | 372.16 | 1.3236 | 1.5676 |
| 29.917 | 72 | 597.01 | 341.65 | 303.71 | 366.12 | 1.3407 | 1.5467 |
| 30.52 | 73 | 563.86 | 373.11 | 311.12 | 357.18 | 1.3646 | 1.5163 |

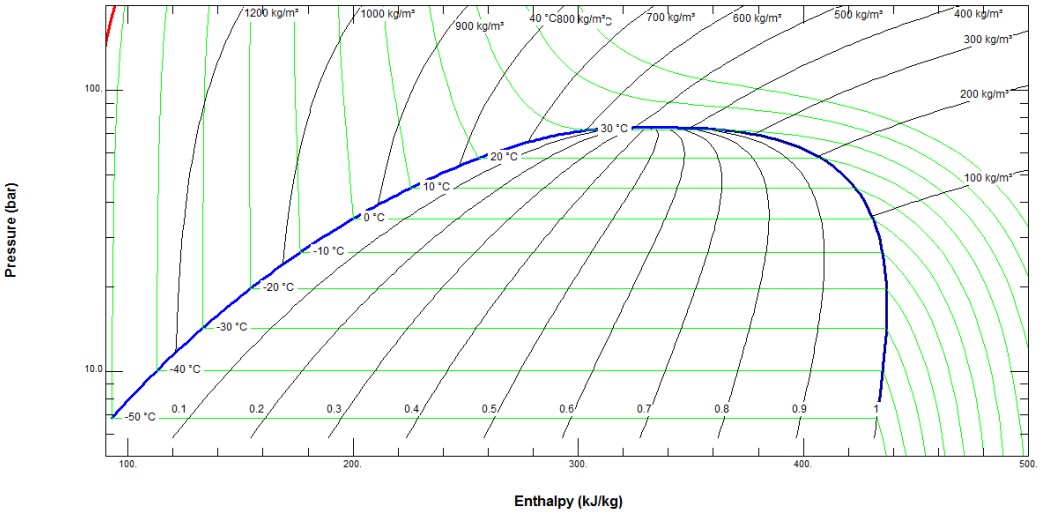


**Figure 11: p-h diagram for $CO_2$ [16].**

# Appendix C: Sample size for pass/fail estimates

The probability to get exactly $n_f$ failures in a sample of $n$ components, which all have a failure rate of 1 in $m$ is given by

$$p = \frac{n!}{n_f!(n-n_f)!}\left(\frac{1}{m}\right)^{n_f}\left(1-\frac{1}{m}\right)^{n-n_f}. \quad (1)$$

The total probability to encounter at least one failure in this sample is therefore

$$p = 1-\left(1-\frac{1}{m}\right)^{n}. \quad (2)$$

For $m = n$ this probability tends to 63% for large $n$. To achieve a lower probability for at least one failure in the same sample (size $n$) the failure rate per component needs to be lowered. For example to achieve a 10% probability the individual failure rate needs to be lowered by a factor 10 (e.g. for $n$ = 1,000 the individual failure rate needs to be 1 in 10,000).

Similar arguments can be used to estimate the sample size needed without a fail in a series of pass/fail tests to set a limit of the failure rate with a confidence level of $c$,

$$n = \frac{\ln(1-c)}{\ln\left(1-\frac{1}{m}\right)}. \quad (3)$$

The sample size n needed in case of one failure is the solution to

$$\frac{1-c}{1+\frac{n-1}{m}} = \left(1-\frac{1}{m}\right)^{n-1}. \quad (4)$$

Therefore, a sample size of about $n$ = 23,000 without failure has to be demonstrated for 90% confidence that the failure rate is 1 in 10,000 or below. Similar confidence can be achieved if one failure is found in about 39,000 pass/fail tests (see Table 12).

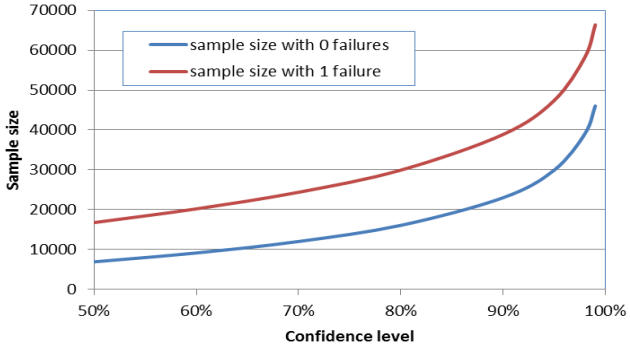


**Figure 12: Required pass/fail test sample size to demonstrate a failure rate of 1 in 10,000 as a function of confidence for no or one failure in the test sample.**

# Appendix D: Standards

## D.1 Standards for pressure equipment

- **EU Pressure Equipment Directive 97/23/EC (PED)** [17]**:** sets out the standards for the design and fabrication of pressure equipment generally over one litre in volume and having a maximum pressure more than 0.5bar gauge. It also sets the administrative procedures requirements for the "conformity assessment" of pressure equipment, for the free placing on the European market without local legislative barriers. However, as the detector cooling system is not produced for commercial resale we can safely ignore these administrative procedures requirements.

  This is enacted in the UK as the Pressure Equipment Regulations (PER).

- **ASME Boiler and Pressure Vessel Code (BPVC)** [18] defined by the American Society of Mechanical Engineers (ASME).

- **PD 5500 (BS 5500):** "Specification for unfired, fusion welded pressure vessels" is a code of practice that provides rules for the design, fabrication, and inspection of pressure vessels.

  PD 5500 was formerly a widely used British Standard known as BS 5500, but was withdrawn from the list of British Standards because it was not harmonized with the European Pressure Equipment Directive (97/23/EC). In the United Kingdom it was replaced by EN 13445. It is currently published as a "Published Document" (PD) by the British Standards Institution.

- **BS EN 13445[5]:** specifies the requirements for design, construction, inspection and testing of unfired pressure vessels. It defines terms, definitions and symbols applicable to unfired pressure vessels. EN 13445 was introduced in 2002 as a replacement for national pressure vessel design and construction codes and standards in the European Union and is harmonized with the Pressure Equipment Directive (97/23/EC or "PED").

## D.2 Standards for tubes and pipe systems

- **BS EN 13480:** Metallic industrial piping. BS EN 13480 is the up-to-date equivalent of the better known BS 5500 which details the calculation and design of metal industrial piping. There are 8 sections in total covering most aspects of metal industrial piping, but only for stainless steel pipes with a limited discussion of aluminium tubes.
  - BS EN 13480-3: This is a long standard of 400+ pages. It provides guidance to calculate pipe wall thicknesses. The most relevant sections are:
    - Section 5 of BS EN 13480-3 covers maximum design stresses in various steel pipes
    - Section 6 of BS EN 13480-3 covers wall calculations for steel pipes
    - Section 10 of BS EN 13480-3 discusses cyclic loading
    - Section 13 of BS EN 13480-3 describes pipe support, but it has nothing to say about the continual constraint we use so is of little help.

[5] National standards identical with the European Norms (EN) are listed with a prefix like BS for British Standard (UK) or DIN for Deutsches Institut für Normierung (Germany). National European standards with the same EN number are identical. Following the colon there is usually a 4 digit year code showing the approval date of the standard (not shown here).

    - BS EN 13480-4: Metallic industrial piping. Fabrication and installation
        - Out-of-roundness at bends

- **BS EN 14276:** This European Standard specifies the requirements for material, design, manufacturing, testing and documentation for stationary pressure vessels intended for use in refrigerating systems and heat pumps. It applies to vessels including welded or brazed attachments up to and including the nozzle flanges, screwed, welded or brazed connectors or to the edge to be welded or brazed at the first circumferential joint connecting piping or other elements. This European Standard applies to pressure vessels with an internal pressure down to - 1 bar, to account for the evacuation of the vessel prior to charging with refrigerant. This European Standard applies to both the mechanical loading conditions and thermal conditions as defined in EN 13445-3 associated with refrigerating systems. It applies to pressure vessels subject to the maximum allowable temperatures for which nominal design stresses for materials are derived using EN 13445-2 and EN 13445-3 or as specified in this standard. In addition vessels designed to this standard should have a maximum design temperature not exceeding 200 °C and a maximum design pressure not exceeding 64 bars. Outside of these limits, it is important that EN 13445 be used for the design, construction and inspection of the vessel.

### 4.10.6 Stainless steel

- **BS EN 10088**: Steel and cast iron standards.
- **ISO 1127:** Stainless steel tubes - Dimensions, tolerances and conventional masses per unit length.

  The outside diameters and thicknesses of the tubes have been selected from ISO 4200. If thicknesses greater than 14.2 mm are needed, they should be chosen from ISO 4200. Specifies the diameters, tolerances and other parameters of tubes. It tabulates conventional masses for austenitic (table 1) and for ferritic and martensitic (table 2) stainless steel tubes.
- **ISO 4200:** Plain end steel tubes, welded and seamless - General tables of dimensions and masses per unit length

  Gives values of both plain end tubes for general purpose use and precision tubes. Its purpose is to give guidance on the selection of sizes for all activities concerned with the standardization of steel tubes, both nationally and internationally, to serve as a ready reckoner and to avoid the use by different countries of different masses for a tube of the same size.
- **BS EN 10216:** Seamless steel tubes for pressure purposes. Technical delivery conditions.
    - Material properties for pressure handling materials
- **BS EN 10217:** Welded steel tubes for pressure purposes.
- **BS EN 13480-3:** Metallic industrial piping. Part 3: Design and calculation
    - Wall thickness calculation for stainless steel tubes and wall thickness at bends

### 4.10.7 Titanium

- **BS EN 4180**: Aerospace series. Circular tubes, for fluids in titanium and titanium alloys. Wide tolerances. Diameter 4 mm ≤ D ≤ 40 mm. Dimensions

- This standard specifies the dimensions and tolerances of circular tubes, for fluids in titanium and titanium alloys for aerospace applications.

### 4.10.8 Aluminium

- **BS EN 573-3:** Aluminium and aluminium alloys. Chemical composition and form of wrought products. Chemical composition and form of products
- **BS EN 754-2:** Aluminium and aluminium alloys. Cold drawn rod/bar and tube. Mechanical properties
- **BS EN 755-1:** Aluminium and aluminium alloys. Extruded rod/bar, tube and profiles. Technical conditions for inspection and delivery
- **BS EN 2070-(series):** Specification for aluminium and aluminium alloy wrought products. Technical specification.
  - **BS EN 2070-5:** Specification for aluminium and aluminium alloy wrought products. Technical specification. Tube used under pressure
    - Design stresses for aluminium alloys
- **BS EN 12392:** Aluminium and aluminium alloys. Wrought products. Special requirements for products intended for the production of pressure equipment
  - Design stresses for aluminium alloys
- **BS EN 13480-8:** Metallic industrial piping. Additional requirements for aluminium and aluminium alloy piping
- Wall thickness calculation for aluminium alloy tube

### 4.10.9 Copper

- **BS 1306:** Specification for copper and copper alloy pressure piping systems
  - Includes wall thickness calculation for copper

## D.3 Welding standards

- BS EN ISO 15614-1:2004+A2:2012 titled “Specification and qualification of welding procedures for metallic materials. Welding procedure test. Arc and gas welding of steels and arc welding of nickel and nickel alloys” (new version presently in work)

# Appendix E: Calculation of wall thickness for stainless steel

Section 4.6.1.1 describes the overall process of specifying the pipes when working with stainless steel. To aid readability the text abridges many aspects and does not contain significant cross referencing. This appendix is intended to fully detail the use of the BS EN standards. The nature of this sort of summary is that it will not be that easy to read, but should comprehensively describe the calculation.

The key European standards for specifying the stainless steel pipe are:

- BS EN 13480-x:2012 (in 8 sections) Specification of pressure piping
- BS EN 10216-5:2013 Material properties for pressure handling materials

At the time of writing (January 2015) the standards listed are the current and most up to date versions.

## E.1 Calculation of wall thickness

For our two candidate pipes we can use the above to compute the required wall thickness *e* for the maximum allowable pressure $P_S$ (130bar$_a$) according to EN13480 (section 6.1) as

$$e = \frac{P_S D_0}{2f \cdot z - P_S}, \tag{5}$$

with the maximum permitted stress *f* and a joint allowance *z*. This equation is the thin wall pipe equation for straight pipes[6]. Thin wall is defined as $D_o/D_i \leq 1.7$ and we expect to have a diameter ratio of approximately 1.2.

## E.2 Calculation pressure

The calculation of the wall thickness in EN13408-3 is based on the calculation pressure, which is defined in section 4.2.3.4 therein:

1. *For all pressure temperature conditions ($p_o$, $t_o$) specified calculation pressures $p_c$ shall be determined.*
2. *The calculation pressure $p_c$ shall be not less than the associated operating pressure $p_o$, taking into account the adjustments of the safety devices.*

For our application the pipe is used only at room temperature and below. Below room temperature the yield rises, so our worst case is room temperature at operating pressure. From the same page, but section 4.2.3.3, we should also note that *Temporary deviations e.g. due to pressure surge or operation of control release valve (safety valve) shall not be taken into account if the calculated stresses from such variations do not exceed the allowable stress by more than 10 % for less than 10 % of any 24 h operating period.*

[6] For a comparison of stress calculations using the thick-wall equations and the thin-wall approximations see Appendix G.

For our calculations we use the maximum allowable pressure as defined in section 3.2 as the operating and the calculation pressure

## E.3 Considerations for the wall thickness calculations

EN 13480 specifies tube dimensions taking three significant factors into account:

1. Maximum allowable stresses in tube wall based upon material and pipe dimensions;
2. Appropriate safety factors;
3. Allowances on wall to allow for fabrication and environmental thinning.

EN 13480 does not make the distinction in these terms, but the more complex structure of the standard can be reduced in this way.

### 4.10.10 Maximum allowable stress and safety factors

For welding Stainless steel pipe we have a preference to use Stainless steel 316L – this is also known as UNS S316xx, and within Europe it is also known as 1.4404 or X2CrNiMo 17.12.2[7] . Properties of 1.4404 appropriate for pressure handling can be found in BS EN 10216-5. The relevant properties from this document are listed in Table 11.

**Table 11: Tensile properties of stainless steel 316L at room temperature from BS EN 10216-5.**

| Steel grade | | Proof strength [MPa] | | | Elongation at failure A [%] | |
|---|---|---|---|---|---|---|
| Steel name | Steel number | 0.2% $R_{p0.2t}$ | 1% $R_{p1.0t}$ | Tensile strength $R_m$ [MPa] | longitudinal | transverse |
| X2CrNiMo17-12-2 | 1.4404 | 190 | 225 | 490 to 690 | 40 | 30 |

These values can be used to calculate the maximum acceptable stress – BS EN13480-3 (section 5.1) tells us that the design stress will be the lower of the time-dependent and time-independent stresses.

### 4.10.11 Time-independent maximum stress

BS EN13480-3 (section 5.2.2) directs us to calculate the maximum permitted strength (*f*). For austenitic steel this is done differently depending on the elongation at failure (*A*). For A=30% (in our pipe transverse is equivalent to hoop stress – the higher load direction)

$$f = \min\left(\frac{R_{p1.0t}}{1.5}, \frac{R_m}{2.4}\right), \tag{6}$$

which yields $f$ = 150 MPa. For A=40% (in our pipe longitudinal is equivalent of axial stress – the lower stress direction)

$$f = \frac{R_{p1.0t}}{1.5}, \tag{7}$$

with the same result.

[7] Stainless 316L is a broader definition than 1.4404 but does include 1.4404.

### 4.10.12 Time-dependent maximum stress

Time dependent stresses capture degradations principally relating to creep, and specifically creep at high temperature. BS EN10216-5 p16 states that non listed materials are not to be used in creep range. This is consistent with information in material datasheets like the Brown metals datasheet (p.10) [19]: "At temperatures of about 1000°F (538°C) and higher, creep and stress rupture become considerations for the austenitic stainless steels". We conclude that below 50˚C we are not in the creep range and so time dependent maximum stress is not a consideration.

We are also not required to provide a safety factor for the welded joints as they are all orbital so implicitly have an additional 100% safety factor compared with the hoop direction yield in the pipe.

From these considerations we conclude that the maximum acceptable stress for use in the tube wall dimensioning is 150 MPa. This compares to a yield strength of 276 MPa and a UTS of 560 MPa and for fully annealed steel. The fully hard yield of 316L stainless steel is above 965 MPa, so we have a factor of 6 before the yield of our material in the fully hard state. The UTS of the fully hard material is above 1280 MPa, so we have a factor of 8.5 before burst.

### 4.10.13 Joint coefficient

BS EN 13408-3 (section 4.5) tells us that no joint considerations are needed for butt welds: *The joint coefficient z shall be used in the calculation of the thicknesses of components which include one or several butt welds, other than circumferential, and shall not exceed the following values…*

We therefore use a joint coefficient of 1 in our calculations.

This is the minimum required pipe wall and will potentially need additions to become a specification.

## E.4 Additional allowances

Specified additions to the calculated wall thickness which need to be considered are:

- Corrosion allowance $C_o$,
- Minimum manufacturing tolerance $C_1$,
- Thinning allowance (from bends) $C_2$.

### 4.10.14 Corrosion allowance

As we are designing for a non-corroding working fluid and for an application in a non-corroding environment we set the corrosion allowance to 0.

### 4.10.15 Minimum manufacturing tolerances

We will specify our tubes wall dimension with a zero lower tolerance. We will perform batch testing of supplied cooling tubes and only accept tubing satisfying this lower limit. We therefore use am manufacturing tolerance allowance of 0.

### 4.10.16 Allowances for bends

Instructions for calculating bend allowances are given in BS EN 13480-3 (section 6.2). There are 3 routes available to calculate wall changes on bends – as there is a free choice between methods we take the "normal route". For this calculations are needed on the internal and external wall dimension in the bends which are specified in BS EN 13480 (section 6.2.3.1) as

$$e_{int} = e\frac{(R/D_0)-0.25}{(R/D_0)-0.5} \text{ and } e_{ext} = e\frac{(R/D_0)+0.25}{(R/D_0)+0.5}. \quad (8)$$

The relevant dimension change is on the outside, where thinning occurs. To maintain the required thickness we need to have enough wall thickness on the straight tube so that the thinned tube in the bend still satisfies the stress calculation from eq. (5). We therefore need to increase this thickness to

$$e_{bend} = e\frac{(R/D_0)+0.5}{(R/D_0)+0.25}. \quad (9)$$

# Appendix F: Calculation of wall thickness for titanium

As there is no guidance in the EN for the dimensioning of titanium tubes we use the ASME Boiler and Pressure Vessel code. This standard is extremely large and complex (16 thousand pages). Here we will only consider a few aspects of it. This whole section refers to "Section VIII Division 1 – Rules for construction of pressure vessels" except where stated otherwise.

Section UG-27 (P20) of the code discusses the thickness of shells under internal pressure (pipes). It states the minimum wall thickness $w_{min}$ defined by the hoop loads as

$$w_{\min} = \frac{pR_i}{SE - 0.6p} \tag{10}$$

with the joint efficiency *E* and the maximum allowable stress *S*. This equation is comparable to our eq. (5) from EN 13480 for stainless steel.

The standard specifies that the joint efficiency of both, radial and axial welds, need to be considered. Should the circumferential welds have too low a joint efficiency (<0.5) the axial load could dominate. Seamless pipe as we are proposing to use has a longitudinal joint efficiency of 1. Further detail can be found in Section UG-27 (P20) of the ASME code. All our proposed joints are circumferential (orbital welds).According to section UW-13 (p117/118) in the ASME code a butt weld from one side made without backing (known as a type 3 weld), has a joint efficiency *E*=0.6 regardless of inspection regime. This is above the limit specified above and therefore we use a joint efficiency of 1.

Section UG-8 (P9) in the ASME BPV code describes maximum stresses and references UG-23 (P17) for non-ferrous materials. The details of these are listed in UNF-23 (P197). This section lists materials by material classification (UNS number). The maximum stresses for our grade of Titanium (UNS R50400), in seamless pipe form (SB-337), are can be found in sub part 1 of section II, part D (listed here in Table 12). As we are working below the lowest temperature listed we are directed to use the material properties from the lowest tier of the table. The tabulated values appear low at first glance (the UTS of CP2 Titanium is 345 MPa, using 86.1 MPa, as required by the standard gives a factor of 4 between working stress and UTS) but like EN13480 they include the safety factors which guarantee that the pipe are kept away from yield.

**Table 12: Yield stress and maximum allowable stress for Titanium in the ASME BPV code [] (our conversions).**

| Material form and Spec no. | ASTM grade | Specified Tensile strength [MPa] | Min Yield 0.2% Offset [MPa] | Maximum allowable stress [MPa] for metal temperature not exceeding | | | |
|---|---|---|---|---|---|---|---|
| | | | | 38°C | 66°C | 93°C | 121°C |
| Pipe SB-337 Seamless | 2 | 345 | 276 | 86.1 | 82.6 | 75.1 | 68.1 |

It should be noted that as with the EN standards the wall thickness from these calculations is defined as a minimum wall thickness, and should in principle be the minimum thickness after corrosion allowances and minimum material manufacturing tolerances. Using similar arguments as in Appendix E we set these allowances to 0.

Finally it should be noted that section UG-16 in the ASME BPV code specifies minimum material thickness in any material section for any shells exclusive of corrosion allowance to be 1.5mm. As we are investigating very small tube wall thicknesses to limit multiple scattering material we are

therefore always in breach of this code. However, there is no fundamental reason why eq. (3) should not apply for smaller wall thicknesses other than weakening due to finite grain size.

# Appendix G: Comparison of thick-wall calculation and thin-wall approximation

Both EN13480 and the ASME BPV code classifies tube definitions in *thick* and *thin* walls. Whilst the standard makes it clear that our pipes are thin-wall it is interesting to compare the data and results from both sets of equations to convince ourselves it is a justifiable approximation.

Stress in tubes can be calculated using Lamé's equations

$$\sigma_{hoop} = \frac{\Delta p D_i^2}{(D_i + 2w)^2 - D_i^2},\ \sigma_{axial}(r) = \frac{\Delta p R_i^2 (R_o^2 + r^2)}{r^2 (R_o^2 - R_i^2)} \text{ and } \sigma_{radial}(r) = \frac{\Delta p R_i^2 (R_o^2 - r^2)}{r^2 (R_o^2 - R_i^2)}, \quad (11)$$

for a pressure differential $\Delta p$, inner and outer diameters $D_i$ and $D_o$ and inner and outer radii $R_i$ and $R_o$, the mean radius $R_{mean}$ and the wall thickness $t$. The von Mises stress is then

$$\sigma_{von\,Mises} = \sqrt{\frac{1}{2}\left((\sigma_{hoop} - \sigma_{axial})^2 + (\sigma_{hoop} - \sigma_{radial})^2 + (\sigma_{axial} - \sigma_{radial})^2\right)}. \quad (12)$$

For thin-walled pipes these equations simplify to

$$\sigma_{hoop} = \frac{\Delta p (R_{mean} - w)}{2w},\ \sigma_{axial} = \frac{\Delta p (R_{mean} - w)}{w}, \text{ and } \sigma_{von\,Mises} = \sqrt{\sigma_{hoop}^2 - \sigma_{hoop}\sigma_{axial} + \sigma_{axial}^2}. \quad (13)$$

We have evaluated these equations for representative dimensions and pressure (Table 13). In all three cases listed EN 13480 and the ASME code specify we should use the thin wall calculations.

As can be seen the thin-wall equations give very close approximation to the thick wall pipe equations (within 15%). Note that the thick wall equation looks at the pipe bore where the highest stressed are expected. The discrepancies are well contained within the safety margins the EN and ASME standards are providing.

**Table 13: Comparison of stresses calculated using the thin and the thick wall approximations.**

| | | | Thin wall | | | Thick wall | | | | Ratio thick/thin | | |
|---|---|---|---|---|---|---|---|---|---|---|---|---|
| OD [mm] | t [mm] | Pressure [$bar_g$] | $\sigma_{hoop}$ [MPa] | $\sigma_{axial}$ [MPa] | $\sigma_{Von\ Mises}$ [MPa] | $\sigma_{hoop}$ [MPa] | $\sigma_{axial}$ [MPa] | $\sigma_{radial}$ [MPa] | $\sigma_{Von\ Mises}$ [MPa] | Hoop | Axial | Von Mises |
| 2.000 | 0.10 | 130 | 55.325 | 110.500 | 95.696 | 55.421 | 123.842 | 13.000 | 96.868 | 100% | 89% | 99% |
| 3.175 | 0.14 | 130 | 63.955 | 127.911 | 110.774 | 64.105 | 141.211 | 13.000 | 111.792 | 100% | 91% | 99% |
| 3.175 | 0.22 | 130 | 37.153 | 74.307 | 64.352 | 37.395 | 87.791 | 13.000 | 66.062 | 99% | 85% | 97% |

The comparison above is illustrative and should not be used for design, should a more creative approach (i.e. EN or ASME codes are not applicable) be needed for component design. BS EN 13445-3 Annex B and C describe a process of design by analysis. BS EN 13445 favours the Tresca yield criterion over Von Mises.

## Acknowledgements

Ian Dawson, Andy Nichols, Jason Tarrant (or author?), Stefano Sgobba, Bart Verlaat (to be completed)

# References


[1] R. Bates et al., *Evaporator and type I cooling tubes and their connections for the ATLAS phase II barrel strip tracker - Part II: Bending and Joining*,

[2] R. Bates et al., *Evaporator and type I cooling tubes and their connections for the ATLAS phase II barrel strip tracker - Part III: Implementation and Verification*,

[3] G. Beck et al., *Phase 2 LOI Backup Document - Thermo-mechanical Local Support - Barrel Stave*, ATL-UPGRADE-PUB-2013-010 (2013).

[4] G. Viehhauser, *ATLAS upgrade ID cooling system requirements*, ATU-SYS-ES-0004 v.5, EDMS 986954 v.5 (2009).

[5] The ATLAS collaboration, *Letter of Intent for the Phase-II Upgrade of the ATLAS Experiment*, CERN-LHCC-2012-022, LHCC-I-023, (2013).

[6 ] B. Verlaat et al., *Design, manufacture and test results of the VCTS $CO_2$ Evaporator for the LHCb experiment at CERN*, 7th International Conference on Heat Transfer, Fluid Mechanics and Thermodynamics (HEFAT2010).

[7] B. Verlaat, *Piping and Instrumentation for the Atlas IBL $CO_2$ cooling system*, ATU-SYS-ES-0018 v.3, EDMS 1233482 v.3. Note that the specification of the evaporator proof pressure in this document is inconsistent with the MAWP and the safety factors described in the text. This is because the stave tube design has been fixed before the overall system pressure requirements have been defined.

[8] http://actiwiz.web.cern.ch/

[9] ATLAS Letter of Intent Phase-II Upgrade, CERN-2012-022, page 60

[10] *The Use of Plastic and other Non-Metallic Materials at CERN with respect to Fire Safety and Radiation Resistance*, CERN TIS IS 41, 3/95.

[11] K. Glitza, *CF stave: CF pipe, Ti/CF joint*, https://indico.cern.ch/event/75802/session/1/contribution/7/material/slides/ .

[12] For a good overview of these methods see J. Moreno Quibén, "Experimental and analytical Study of two-phase pressure drops during evaporation in horizontal tubes", Thése N° 3337 (2005), Lausanne EPFL, http://library.epfl.ch/theses/?display=detail&nr=3337.

[13] L. Cheng, G. Ribatski, J. Moreno Quibén and J.R. Thome, *New prediction methods for $CO_2$ evaporation inside tubes: Part I – A two-phase flow pattern map and a flow pattern based phenomenological model for two-phase flow frictional pressure drops*, Int. J. Heat Mass Transf. 51 (2008) 111-124.

L. Cheng, G. Ribatski and J.R. Thome. *New prediction methods for $CO_2$ evaporation inside tubes: Part II – An updated general flow boiling heat transfer model based on flow patterns*, Int. J. Heat Mass Transf. 51 (2008) 125-135.

J.R. Thome and J. El Hajal, *Flow boiling heat transfer to carbon dioxide: general prediction method*, Int. J. Refr. 27 (2004) 294-301.

[14] L. Friedel, *Improved friction drop correlations for horizontal and vertical two-phase pipe flow*, Proc. European Two-phase Flow Group Meeting, paper E2, JRC-Ispra, Italy, 1979.

[15] J.C. Chen, *Correlation for boiling heat transfer to saturated liquids in convective flow*, Int. Eng. Chem. Process Design and Development 5 (1966) 322.

[16] REFPROP.

[17] *EU Pressure Equipment Directive 97/23/EC (PED)*, http://eur-lex.europa.eu/legal-content/EN/TXT/PDF/?uri=CELEX:01997L0023-20130101&from=EN.

[18] ASME Boiler and Pressure Vessel Code (BPVC)

[19] http://www.brownmetals.com/downloads/Alloy316TechSheet.pdf